

A HEAT BUDGET FOR CANYON RESERVOIR, A SUBTROPICAL
IMPOUNDMENT IN SOUTHCENTRAL TEXAS

THESIS

Presented to the Graduate Council of
Southwest Texas State University
In Partial Fulfillment of
The Requirements

For the Degree

Master of SCIENCE

By

David A. Bass, B.S.

San Marcos, Texas
December 2000

ACKNOWLEDGEMENTS

Thanks are given to the Biology faculty and Aquatic Biology graduate students who have helped see my graduate studies to completion. I especially thank Dr. Alan Groeger for his patience and guidance in both my graduate studies at Southwest Texas State University and this undertaking. I also thank my parents for their support and encouragement to further my education.

TABLE OF CONTENTS

	Page
LIST OF TABLES	vi
LIST OF FIGURES	vii
ABSTRACT	ix
CHAPTER	
I. INTRODUCTION	1
II. METHODS	6
III. RESULTS AND DISCUSSION	15
APPENDICES	
A. CONVERSION FACTORS AND SYMBOLS USED	49
B. SOLAR RADIATION CALCULATION	52
C. OUTFLOW TEMPERATURE CALCULATION	55
D. ATMOSPHERIC ATTENUATION COEFFICIENT CALCULATION	58
E. SUMMARY STATISTICS USED TO DEVELOP THE HEAT BUDGET FOR CANYON RESERVOIR	60
BIBLIOGRAPHY	69

LIST OF TABLES

Table	Page
1. Morphometric characteristics of Canyon Reservoir	6
2. General flow regime for Canyon Reservoir for 1969-99	20
3. Comparison of the individual heat budget component's 31-yr means to the three driest and three wettest years in Canyon Reservoir's history	47
4. Intercepts, slopes and descriptive statistics from the regression equations for predicting outflow temperatures of Canyon Reservoir	57
5. Atmospheric attenuation coefficients for each month used to calculate atmospheric long wave input into Canyon Reservoir.....	59

LIST OF FIGURES

Figure	Page
1. Annual variability within some of the meteorological variables used to determine the heat budget of Canyon Reservoir	17
2. Mean annual wind speed at San Antonio, Texas	18
3. Mean monthly inflows and outflows of Canyon Reservoir 1969-1999	19
4. Monthly heat input, output and net gain through advection in Canyon Reservoir 1969-1999	23
5. Mean monthly net heat gain through advection	24
6. Percent contribution by month of advection to the net heat budget of Canyon Reservoir	25
7. Mean monthly amount and variability of heat gain through solar radiation 1969-1999	27
8. Mean monthly amount and variability of heat gain through atmospheric long wave radiation 1969-1999.....	29
9. Net solar and atmospheric long wave radiation heat input in Canyon Reservoir 1969-1999	30
10. Mean monthly amount and variability of heat loss through water long wave back radiation 1969-1999	32

11. Mean monthly amount and variability of heat loss through evaporation 1969-1999	34
12. Mean monthly amount and variability of heat loss through conduction 1969-1999	35
13. Heat loss due to conduction, evaporation and water long wave back radiation over the history of Canyon Reservoir 1969-1999	36
14. Heat input, output and net gain for the surface flux components of the heat budget of Canyon Reservoir	38
15. Monthly heat gain through surface flux, advection and net balance in Canyon Reservoir 1969-1999	39
16. Generalized annual heat budget of Canyon Reservoir	41
17. Generalized monthly heat budgets for the advective and surface flux components of the heat budget of Canyon Reservoir	42
18. Monthly heat gain through surface flux, advection, and net balance 1990-1993	45

ABSTRACT

A HEAT BUDGET FOR CANYON RESERVOIR, A SUBTROPICAL IMPOUNDMENT IN SOUTHCENTRAL TEXAS

by

David A. Bass, B.S.
Southwest Texas State University
December 2000

Annual heat budgets were constructed for a subtropical (30°N) reservoir over its 31-year history and used to examine the influence of local climatic variability on hydrological and thermal processes. Heat balances were calculated using both observed and derived hydrological and meteorological data, and some of the heat flux equations were modified to more accurately reflect the local climate. During this study period, surface heat exchange accounted for 67% of the annual heat flux. The magnitude and patterns of surface heat fluxes observed at Canyon Reservoir were intermediate between those of tropical and temperate lakes. The reservoir showed the sinusoidal pattern of heat gain seen in temperate lakes, but the amount of heat flux was more similar to tropical reservoirs. The climate of southcentral Texas is quite variable, and over its history Canyon Reservoir has experienced several major floods and droughts, providing insight into the role advection plays in reservoir heat dynamics. The reservoir acted as a trap for advected heat. The contribution advected heat made to the total heat budget

averaged 33%, but varied from < 1% to > 95% depending on the volume of water entering the reservoir and time of year. To further explore the role advection played in Canyon Reservoir's heat dynamics, data on the three wettest and driest years were compared. Net heat balances were quite different between the two groups of years. In the driest years, the reservoir lost $52 \text{ cal cm}^{-2} \text{ d}^{-1}$ more heat than the 31-yr mean, making the reservoir an overall heat source to its environment. During the wettest years, the reservoir gained $19 \text{ cal cm}^{-2} \text{ d}^{-1}$ more heat than the 31-yr annual mean, increasing its role as a heat trap.

CHAPTER I

INTRODUCTION

Most of the chemical, physical and biological functions in an aquatic ecosystem either are controlled or greatly influenced by the movement and temperature of water (Hostetler 1995). Because climate is the primary determinant of local runoff and temperature, lacustrine ecosystems are sensitive to long-term climatic variability and change.

The effects of climate change have been shown to influence almost all of the processes occurring in lakes and reservoirs. Fee et al. (1996) found that increased CO₂ levels would reduce precipitation resulting in the reduction of the amount of dissolved organic carbon (DOC) entering into aquatic ecosystems. Reduced DOC inputs should increase reservoir transparency, and this increased transparency would deepen the epilimnion allowing for changes in nutrient recycling efficiency, the vertical distribution of biota in the water column, and the amount of photosynthetically available irradiance.

Schindler et al. (1996) examined the properties of lakes in northwest Ontario, and found significant changes in water temperature (increase), pH (increase), thermocline depth (increase), and chemical transport rates (decrease) in recent years. Most of these changes were related to climatic warming resulting in lower amounts of precipitation and higher temperature and evaporation rates. Hambright et al. (1994), also found increasing thermocline depth and increased nutrient regeneration (phosphorus) in a subtropical lake, but these effects were attributed to a gradual decrease in winter air temperature. DeStasio et al. (1996) suggested that the duration and frequency of hypolimnetic anoxia could increase with climatic warming. Increased periods of anoxia would change nutrient recycling rates and increase the nutrient content of the water column.

One tool that can be used to analyze climatic influences on lakes and reservoirs is the construction of a heat budget (Hostetler 1995). A heat budget has two main components. The first is advective heat gain, which can be quantified as the heat content of inflowing minus that of outflowing water. Advection is defined as the transport of material by water movement. The second component is surface heat flux within the reservoir. This value is the sum of heat gained through atmospheric and solar input minus the heat loss through back

radiation, evaporation and conduction. When these two elements are combined the result is a model of thermal dynamics that provides insight into how physical processes in a reservoir influence the structure of the ecosystem and its chemical and biological characteristics.

Since heat is carried into and out of a reservoir by advection, water movement through the reservoir becomes an important hydrological characteristic to consider when describing lacustrine ecosystem structure. One measure of water movement through a reservoir is residence time (Horne and Goldman 1994). In addition to its importance to physical processes, water residence time, or advective movements, influences other aspects of the reservoir ecosystem.

The importance of residence time to the productivity and stability of reservoirs has been examined in a number of earlier studies. Townsend et al. (1996) reported that light attenuation and color were inversely related to residence time in two tropical reservoirs. Light attenuation determines the maximum depth of photosynthesis, and therefore, can be a major determinant of primary productivity in reservoirs. Groeger and Kimmel (1984) found a similar relationship between organic matter supply and water residence time, but a

positive relationship between organic matter retention efficiency and water residence time. Because organic matter is the energy base for water bodies, changes in loading, retention and processing influence their food web structure and secondary productivity. Water residence time also influences reservoir water column stability (Johnson et al. 1978). The timing and intensity of changing residence times (e.g., floods) can shift the onset and break down of stratification (Ford 1990, Groeger and Tietjen 1998). Thermal and density gradients and hypolimnetic dissolved oxygen concentrations are sensitive to differing residence times in Canyon Reservoir (Groeger and Tietjen 1998).

Water residence can also be important in controlling nutrient dynamics. Nutrient retention and transformation are directly affected by the flushing effect during periods of short residence time (Turner et al. 1983). Increased water velocity and physical mixing characteristic of high flow conditions does not allow particulate matter settle out of the water column as in times of low flow. Nutrient loading has been directly related to the magnitude of inflows (Vollenweider 1976), as more material is transported into the lake. Schindler et al. (1996) found that the concentration of inorganic chemical constituents within boreal lakes increases with increasing water residence times and that these increases were

attributable to in-lake processes. Water residence time, therefore, is an extremely important variable in determining structure and function in reservoir ecosystems.

The primary objective of this study was to construct annual heat budgets over the history of Canyon Reservoir in order to examine the influence of climatic variability on hydrological and thermal processes. Additionally, these budgets provide a way to examine the role advection plays in reservoir heat dynamics and ecosystem structure.

CHAPTER II

METHODS

Study area

Canyon Reservoir is a hardwater, oligo-mesotrophic deep-draining reservoir located on a fourth order segment of the Guadalupe River in southcentral Texas (N 29° 52', W 98° 12'). Table 1 lists Canyon Reservoir's catchment, storage and morphometric characteristics.

Table 1. Morphometric characteristics of Canyon Reservoir.

Conservation pool elevation	277 m asl
Outlet elevation	236 m asl
Volume at conservation pool	$4.71 \times 10^8 \text{ m}^3$
Mean depth	14.3 m
Maximum depth	48 m
Drainage basin size	3709 km^2
Area at conservation pool elevation	33.4 km^2

Heat budget calculations

The amount of advective heat gained in a reservoir is dependent on the temperature and volume of inflowing and outflowing waters. Inflowing water

temperature and volume is usually controlled by regional climatic and hydrological conditions, while a reservoir's discharge frequency and volume is often dependent upon the purpose the reservoir serves and its management scheme (Owens et al. 1998). Advective heat gain is relatively straightforward to ascertain and can be calculated as:

$$\text{Advective heat gain (cal)} = (Q_{in})(\rho)(T_{in})(C_p) - (Q_{out})(\rho)(T_{out})(C_p) \quad (1)$$

where Q_{in} = discharge into the reservoir ($\text{m}^3 \text{s}^{-1}$),

Q_{out} = discharge from the reservoir ($\text{m}^3 \text{s}^{-1}$),

T_{in} = temperature of inflowing water ($^{\circ}\text{C}$),

T_{out} = temperature of outflowing water ($^{\circ}\text{C}$),

ρ = density of water at temperature T (kg m^{-3}), and

C_p = specific heat of water ($\text{cal g}^{-1} \text{ }^{\circ}\text{C}^{-1}$).

Surface heat flux can be determined in several ways (Edinger et al. 1968, Ragotzkie 1978, Johnson et al. 1978, Chapra 1997, Townsend et al. 1997, Owens 1998, Allen et al. 1998), but each of these methods have several components in common: incoming short wave radiation, incoming long wave radiation from the atmosphere, back radiation from the water, evaporative losses,

and conduction of heat to or from the reservoir's surface. Collectively, these terms address heat gain or loss within the body of a reservoir. The terminology and symbols I used are taken from Chapra (1997). All symbols and conversion factors used in this paper are located in Appendix A.

Net solar short wave radiation (J_{sn} , $\text{cal cm}^{-2} \text{d}^{-1}$) is dependent on the time of day and year, the sun angle, atmospheric attenuation, the latitude of the water body and the albedo of water (Ragotzkie 1978). This value can either be calculated (Allen et al. 1998, Owens et al. 1998) or directly measured using pyrheliometers.

The sources of long wave radiation from the atmosphere (J_{an}) are direct solar input and from short wave solar radiation and reflected radiation from the earth that has been absorbed by the atmosphere (via clouds) and re-emitted as infrared. J_{an} is calculated by the following equation:

$$J_{an} (\text{cal cm}^{-2} \text{d}^{-1}) = \sigma(T_{air} + 273)^4(A + 0.031\sqrt{e_{air}})(1 - R_L) \quad (2)$$

where σ = Stefan-Boltzmann constant ($11.7 \times 10^{-8} \text{ cal cm}^{-2} \text{d}^{-1} \text{ } ^\circ\text{K}^{-4}$),

T_{air} = air temperature ($^\circ\text{C}$),

A = atmospheric attenuation coefficient (dimensionless),

R_L = reflection coefficient (dimensionless), and

e_{air} = saturation vapor pressure of the overlying air (mm Hg),

where $e_{\text{air}} = 4.596e^{\frac{17.27 T_d}{237.3 + T_d}}$ (3)

with T_d = dew point temperature ($^{\circ}\text{C}$).

Because water behaves as a near perfect black body (Ragotzie 1978), it emits long wave radiation. This form of heat loss is termed (J_{br}), and is calculated as:

$$J_{\text{br}} (\text{cal cm}^{-2} \text{ d}^{-1}) = \varepsilon \sigma (T_s + 273)^4 \quad (4)$$

where ε = emissivity of water (dimensionless), and

T_s = water surface temperature ($^{\circ}\text{C}$).

Evaporative heat loss (J_e) is the major non-radiation means of heat loss from natural lakes (Ragotzkie 1978). Evaporation is controlled by air movement and vapor pressure gradients across the air-water interface. The calculation of heat loss due to evaporation can be expressed as :

$$J_e (\text{cal cm}^{-2} \text{ d}^{-1}) = f(U_w)(e_s - e_{\text{air}}) \quad (5)$$

where $f(U_w)$ = function defining the relationship between wind

velocity over the water's surface and heat transfer. In this

case: $19 + 0.95U_w^2$ where U_w = wind speed (m s^{-1}), and

e_s = saturation vapor pressure at the water's surface

$$\text{(mm Hg) with } e_s = 4.596e^{\frac{17.27 T_s}{237.3 + T_s}} \quad (6)$$

Conduction and convection (J_c) refer to heat transferred across the water's surface. Wind and overlying air stability govern heat transfer through conduction and convection (Ragotzkie 1978), and its role in the overall heat budget is usually small. This component of the surface heat flux can be represented as:

$$J_c \text{ (cal cm}^{-2} \text{ d}^{-1}) = (c_1)f(U_w)(T_s - T_{air}) \quad (7)$$

where c_1 = Bowen's coefficient (0.47 mm Hg °C⁻¹).

These terms combine to give the surface heat flux budget (J_{net}), and can then be expressed as:

$$J_{net} \text{ (cal cm}^{-2} \text{ d}^{-1}) = J_{sn} + J_{an} - (J_{br} + J_c + J_e) \quad (8)$$

When combined, the advective and surface flux components presented above provide a model of the total heat balance of a reservoir. Heat transfer at the sediment-water interface has been ignored in this study, as other authors

have noted that, in water bodies with morphometry similar to that of Canyon Reservoir, sediment heat flux is negligible (Ragotzie 1978, Johnson et al. 1985).

Meteorological and hydrological calculations

Monthly means for air temperature, dew point, wind speed, precipitation and solar radiation at San Antonio, Texas were calculated from daily values using data collected under the National Oceanographic and Atmospheric Administration's (NOAA) Solar and Meteorological Surface Observation Network (SAMSON) program. The SAMSON program collected data from 1961–1990 and the 1991-1999 data were obtained from the National Climatic Data Center (NOAA 1991-1999). These data were used to calculate the terms of the surface heat flux component of the model. Additionally, directly measured net solar radiation values were not available after 1990. These missing data were calculated using methods described by Allen et. al (1998), and the calculations and methodology are described in Appendix B.

Monthly mean area of Canyon Reservoir was calculated for 1969–1999 using a linear regression equation developed from Army Corps of Engineers hypsographic data ($n = 37$, $r^2 = 0.999$), and employed daily reservoir volumes. Area was important in determining the total surface heat content of the reservoir,

as energy flux is usually reported on an areal basis. The regression equation reported area as a function of reservoir volume. Daily reservoir volume data were obtained through USGS online data retrieval system and publications by the US Geological Survey (USGS 1969-1999). Daily noon-time reservoir elevation data were obtained via the Fort Worth, Texas District of the Army Corps of Engineers' online hydrological data retrieval system. These values were condensed into monthly means.

Guadalupe River temperatures above the reservoir near Spring Branch, TX were calculated using a regression equation (Equation 9, $n = 24$, $r^2 = 0.986$, Groeger and Bass in prep) developed using monthly mean air temperatures at Boerne, Texas (N 29° 47', W 98° 44', 433 m asl) and monthly mean river temperatures taken near Spring Branch at USGS station #08167500 using a recording thermistor that collected data at 5-min intervals. Boerne air temperatures were obtained from NOAA published data (NOAA 1969-1999)

$$T_{sb} = 0.91T_b + 3.538 \quad (9)$$

where T_{sb} = Guadalupe River temperature (°C) at Spring Branch,

and

T_b = Air temperature (°C) at Boerne.

Monthly mean water temperatures ($z = 3$ m) in Canyon Reservoir near the dam were estimated using a regression equation (Equation 10) that reported this temperature as a linear function of the previous 30-d mean air temperature at San Antonio ($n = 230$, $r^2 = 0.962$, Groeger and Bass in prep). I assumed this temperature was representative of the entire reservoir's surface temperature.

$$T_{3m} = 0.887(\text{SA30day}_{\text{Temp}}) + 2.527 \quad (10)$$

where T_{3m} = Canyon Reservoir temperature ($^{\circ}\text{C}$) at 3 meters,
 $\text{SA30day}_{\text{Temp}}$ = Mean daily San Antonio air temperature
 for the previous 30 days.

Canyon Reservoir outflow temperatures were calculated using regression equations formulated from mean monthly air temperatures at Boerne, outflow volumes from the USGS and Canyon Reservoir outflow temperature data collected by the Guadalupe-Blanco River Authority. Appendix C provides a summary of the regression equations. All regression equations were developed using SPSS (1998).

Equation 11 was used to calculate water density (ρ), and was taken from Ford and Johnson (1983).

$$\rho = 999.841 + 6.59583 \times 10^{-2}T - 8.45123 \times 10^{-3}T^2 + 5.29159 \times 10^{-5}T^3 \quad (11)$$

where T = water temperature ($^{\circ}\text{C}$).

Once calculated, these values were then expressed as $\text{cal cm}^{-2} \text{d}^{-1}$ in order to allow for comparisons to the other components of the heat budget.

It should be noted that equation 2 contains a coefficient to account for the atmospheric attenuation of long wave radiation. Chapra (1997) recommends a value between 0.50 and 0.70. This range of values does not adequately reflect meteorological conditions for Canyon Reservoir, so more site specific values were derived. Appendix D contains the methods used to derive the coefficient used, as well as the monthly values obtained.

CHAPTER III

RESULTS AND DISCUSSION

Meteorological variables

The climate of southcentral Texas is quite variable both spatially and temporally, but some generalities can be made. Norwine (1995) characterized the regional rainfall variability of south Texas as unusually high when compared to other semiarid regions throughout the world. During this 31-yr study period, the annual precipitation coefficient of variation (C.V.) of 28% at San Antonio is consistent with Norwine's (1995) values. Coefficients of variation for individual monthly precipitation ranged from 68 (May) to 141% (December). During the winter months, precipitation was generally lowest and most variable. Mean annual precipitation during this period was 822 mm, and ranged from 473-1323 mm.

The mean annual air temperature of 20.3°C at San Antonio ranged from 18.9°C to 21.7°C. There is some indication that mean annual air temperature has

increased over this 31-yr study period, but the relationship is not strong ($r^2 = 0.21$). In addition to possible warming, variability in mean annual air temperature, dew point temperature, and precipitation at San Antonio has increased over the latter half of the study period, but Boerne mean annual air temperatures were more constant (Figure 1).

No generalizations concerning mean annual wind speed could be made, as the monitoring station has been relocated and monitoring equipment changed in the mid-1980s. The relocation of the anemometer did not allow for a consistent data set. These effects are evident in Figure 2, though the overall heat budget is little influenced by the change. Summaries of mean monthly values for the meteorological variables used in this model are presented in Appendix E.

Hydrological patterns

The general hydrologic regime of Canyon Reservoir is presented in Table 2 and Figure 3. Discharge from the reservoir generally lagged inflows by 1 month, and monthly reservoir water residence time was inversely related to monthly flow into the reservoir. The lag period is partially the result of reservoir management practices. Through the 31-yr period since reaching conservation pool elevation in 1969, the mean annual water residence time in Canyon

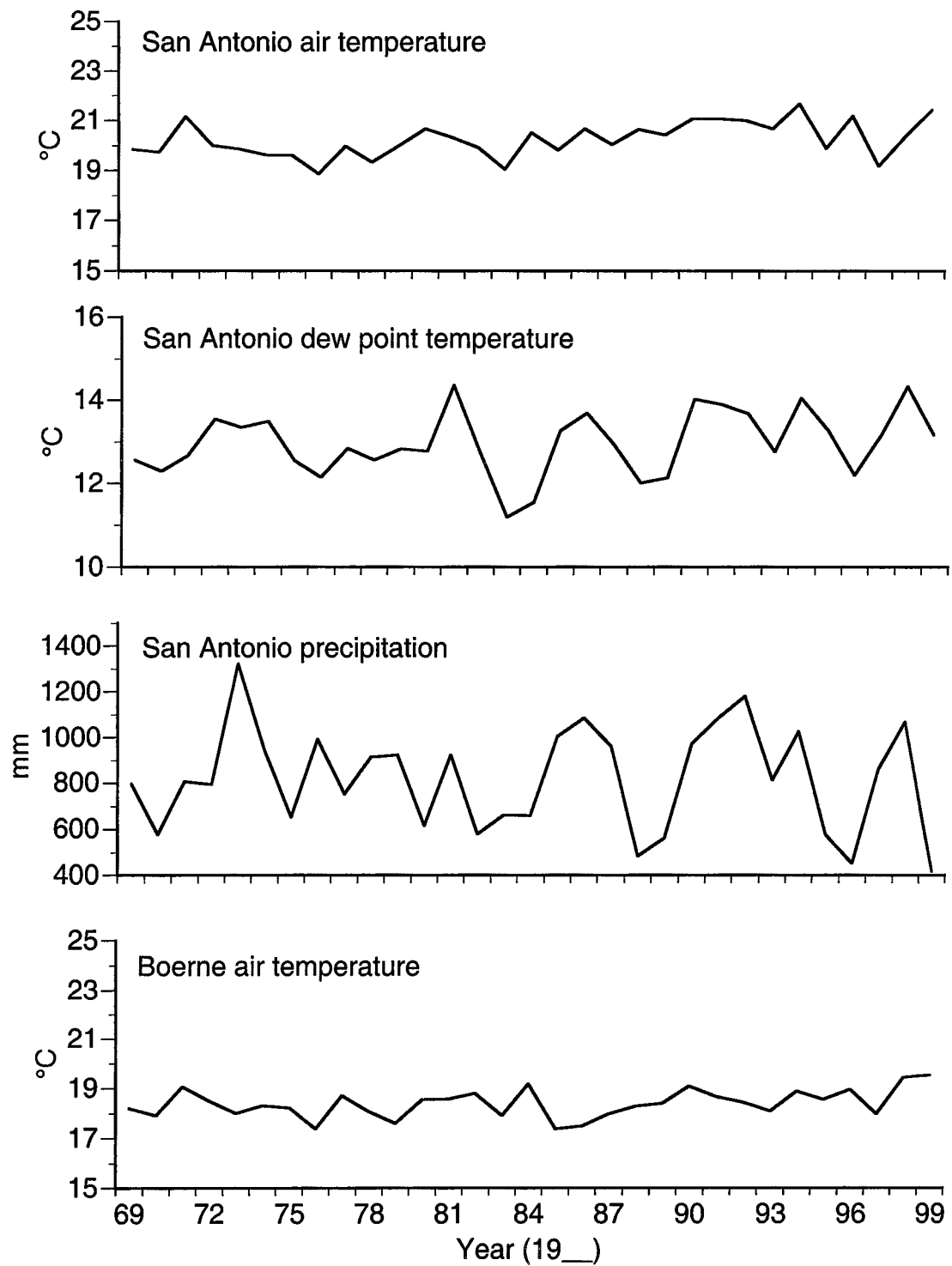


Figure 1. Annual variability within some of the meteorological variables used to determine the heat budget of Canyon Reservoir.

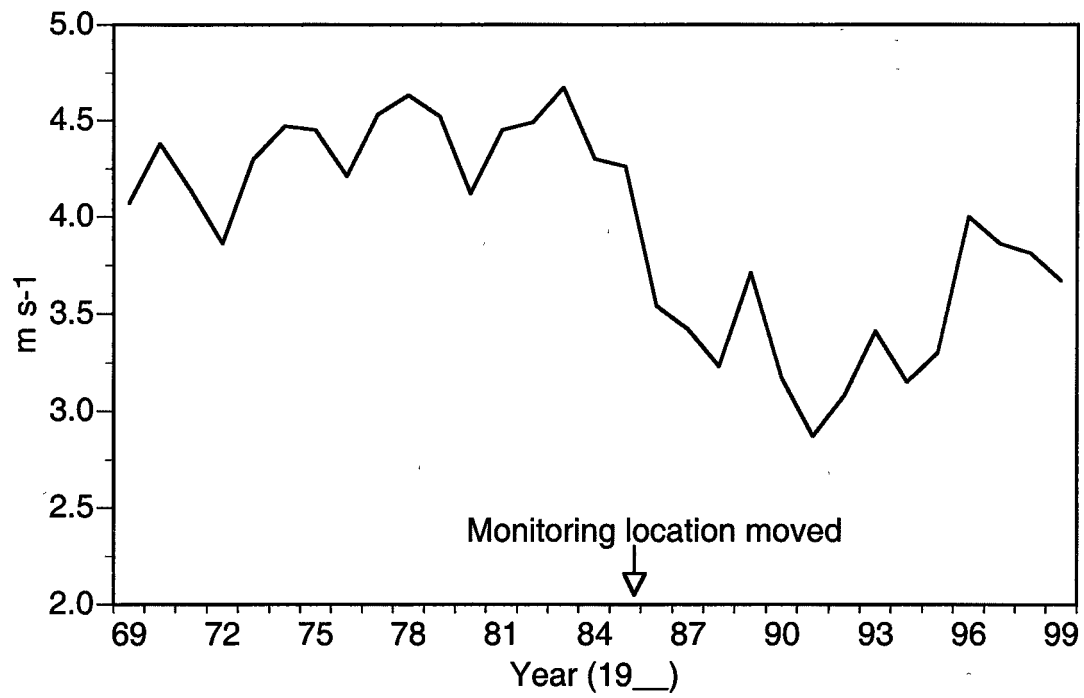


Figure 2. Mean annual windspeed at San Antonio, Texas.

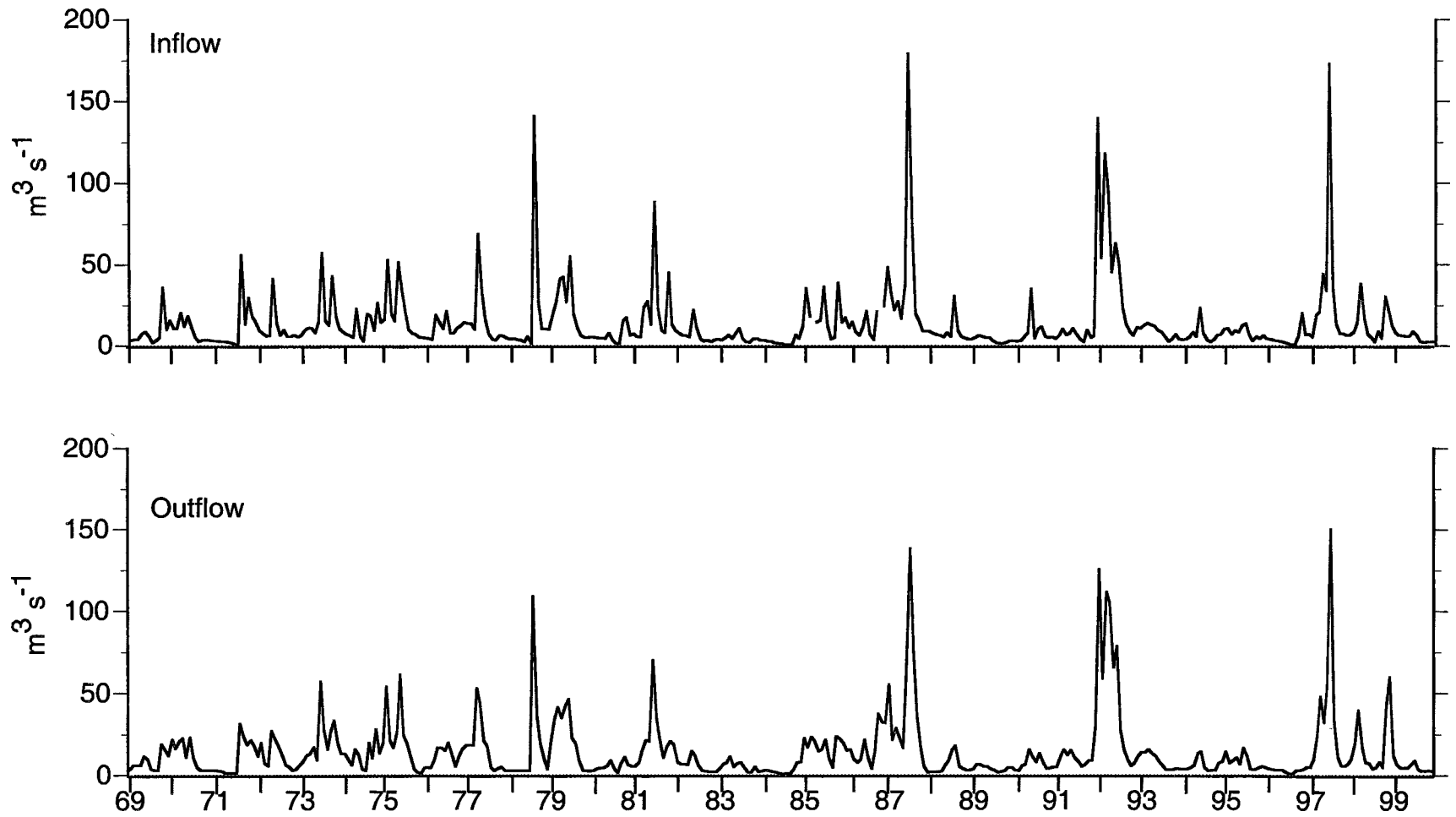


Figure 3. Mean monthly inflows and outflows at Canyon Reservoir 1969-1999.

Reservoir has been 1.61 yr (C.V. = 67%). These annual values hide considerable variability caused by the unpredictability in the magnitude and timing of storms because water residence times calculated on monthly intervals show much more variation (mean = 2.62 yr, C.V. = 97%).

Table 2. General flow regime for Canyon Lake for 1969-99.

<u>Annual</u>	
Mean water residence time	1.61 yr
Range	0.33 - 4.53 yr
Coefficient of variation	67%
<u>Monthly</u>	
Mean water residence time	2.62 yr
Range	0.14 - 20.32 yr
Coefficient of variation	97%

Heat flux through advection

The volume of inflowing water and its temperature are responsible for the amount of heat advected into the reservoir. Although there is extreme variability in precipitation and consequent river inflows in this region, the amount of water entering Canyon Reservoir appears to be seasonal. However, if the 18 months with greatest flows (the upper 5% of individual monthly inflows) are removed, there is no definite seasonality evident. In addition to the influence of spates, seasonal patterns in the amount of heat entering the reservoir through advection are further obscured when the temperature of inflowing water is considered

because the temperature of the inflowing water is not necessarily that of the reservoir.

As with heat entering the reservoir, the volume and temperature of outflowing waters determine the amount of heat leaving the system. Unlike inflows, dam design and management practices determine the volume and temperature of water exiting the reservoir. Reservoirs with outlet structures located in the hypolimnion (such as Canyon Reservoir) tend to act as heat traps for most of the year (Wright 1967). Heat trapping occurs when inflows are warmer than outflows. Because the winter temperature of the reservoir plays a large role in determining the spring hypolimnion temperature and density (Johnson and Ford 1983), heat trapping can have a large influence on the thermal structure of the reservoir. As the year progresses into summer, the hypolimnion becomes increasingly isolated from upper water layers and the atmosphere as density gradients become established. Inflowing water (and heat) enters the reservoir at the depth equivalent to its density, and if these density flows enter the deeper regions of the hypolimnion, the heat carried in will be available for discharge. If density gradients prevent inflowing water from entering the hypolimnion, these inflows are stored in the reservoir while cooler water is

released resulting in net heat gain. Johnson and Merrit (1978) observed this type of flow regime in a temperate reservoir (Lake Powell). The timing of thermocline development, which is driven by interactions between external heat inputs and the stability of local weather conditions (Horne and Goldman 1994), also influences the hypolimnion temperature and heat content.

While heat entering the reservoir is a function of hydrometeorology, heat removed is determined by the reservoir's management practice and the tendency for the reservoir to act as a heat trap. Canyon Reservoir has gained a long-term monthly mean of $15 \text{ cal cm}^{-2} \text{ d}^{-1}$ through advection. Figure 4 presents the advective components of the reservoir's heat budget as well as their balance.

Advected heat is usually lost in the late fall and winter months (November - February), when release water is usually warmer than inflows. Over the rest of the year, however, the reservoir gains heat (Figure 5). The relative importance of advective heat gain varies from less than 1% of the total heat budget up to >95%, depending on the time of year and the monthly flow regime (Figure 6). In February and September, heat flux at the surface approaches zero, so any advected heat will have more importance to the overall heat budget. Likewise,

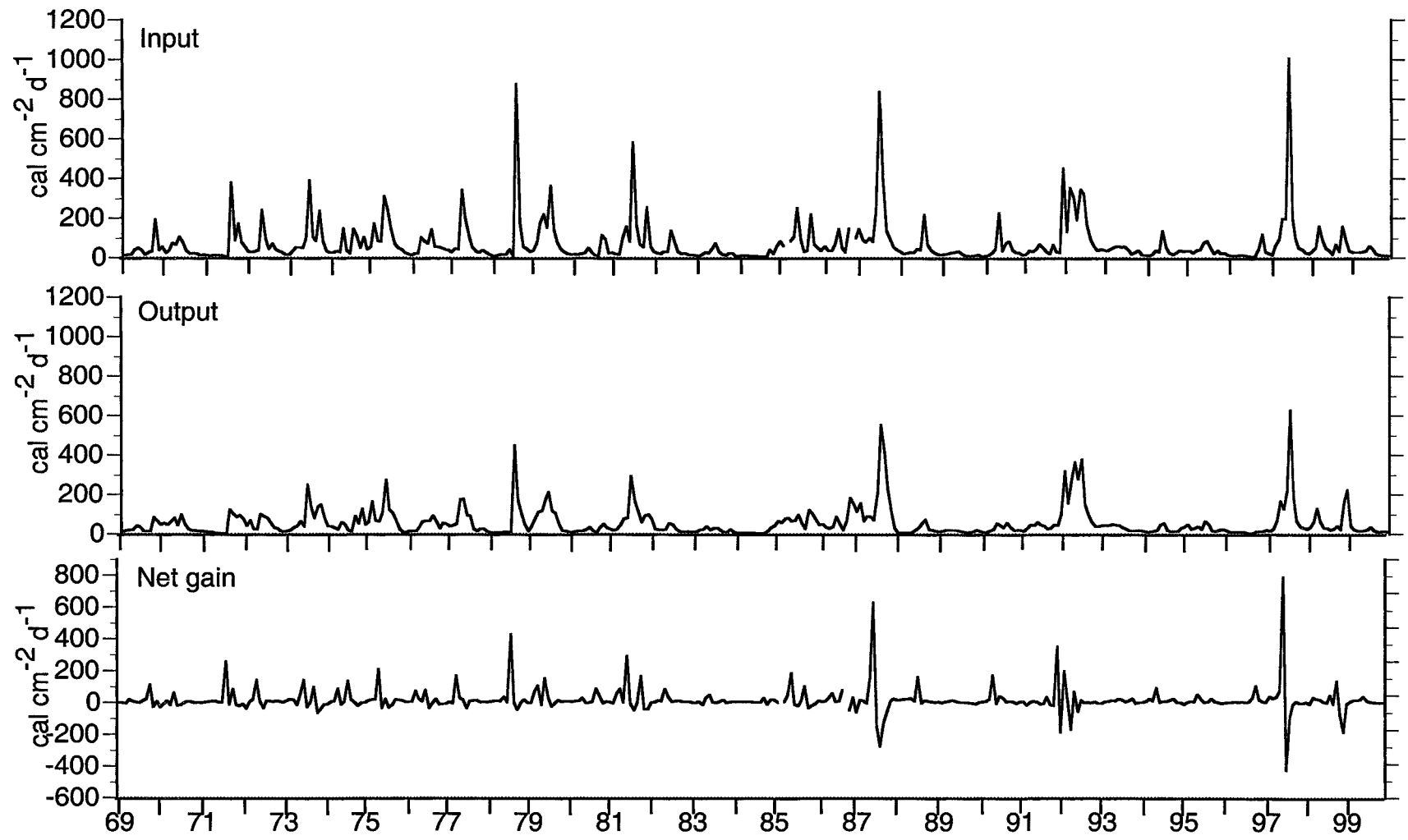


Figure 4. Monthly heat input, output and net gain through advection in Canyon Reservoir 1969-1999.

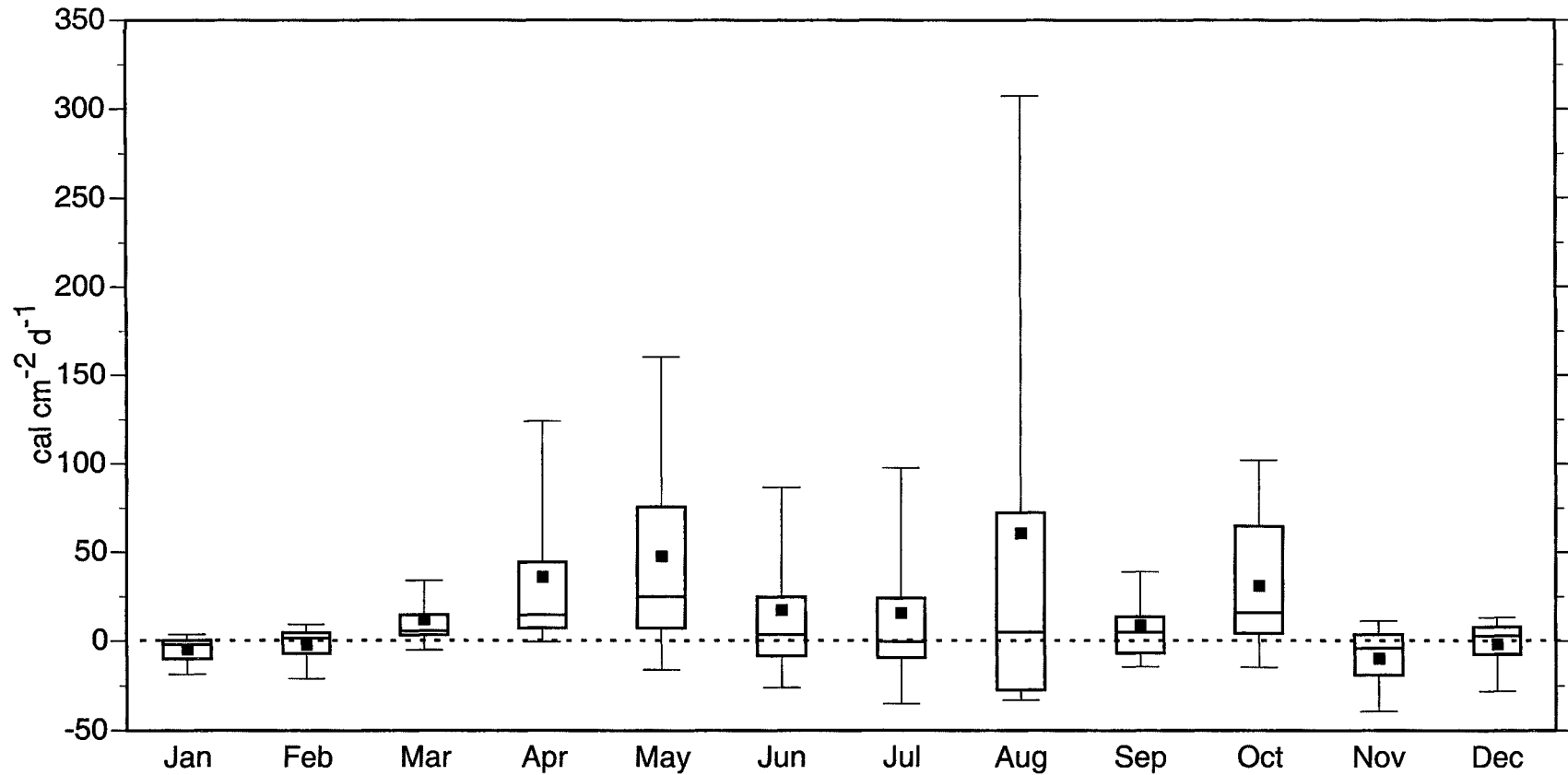


Figure 5. Mean monthly heat gain through advection. For each month, $n=31$ except March ($n=30$) and October ($n=30$). For this and all other box and whisker plots: the whiskers represent the 10th and 90th percentiles, the upper and lower boundaries of the boxes are the 75th and 25th percentiles, the dash within the boxes represent medians and dots represent means.

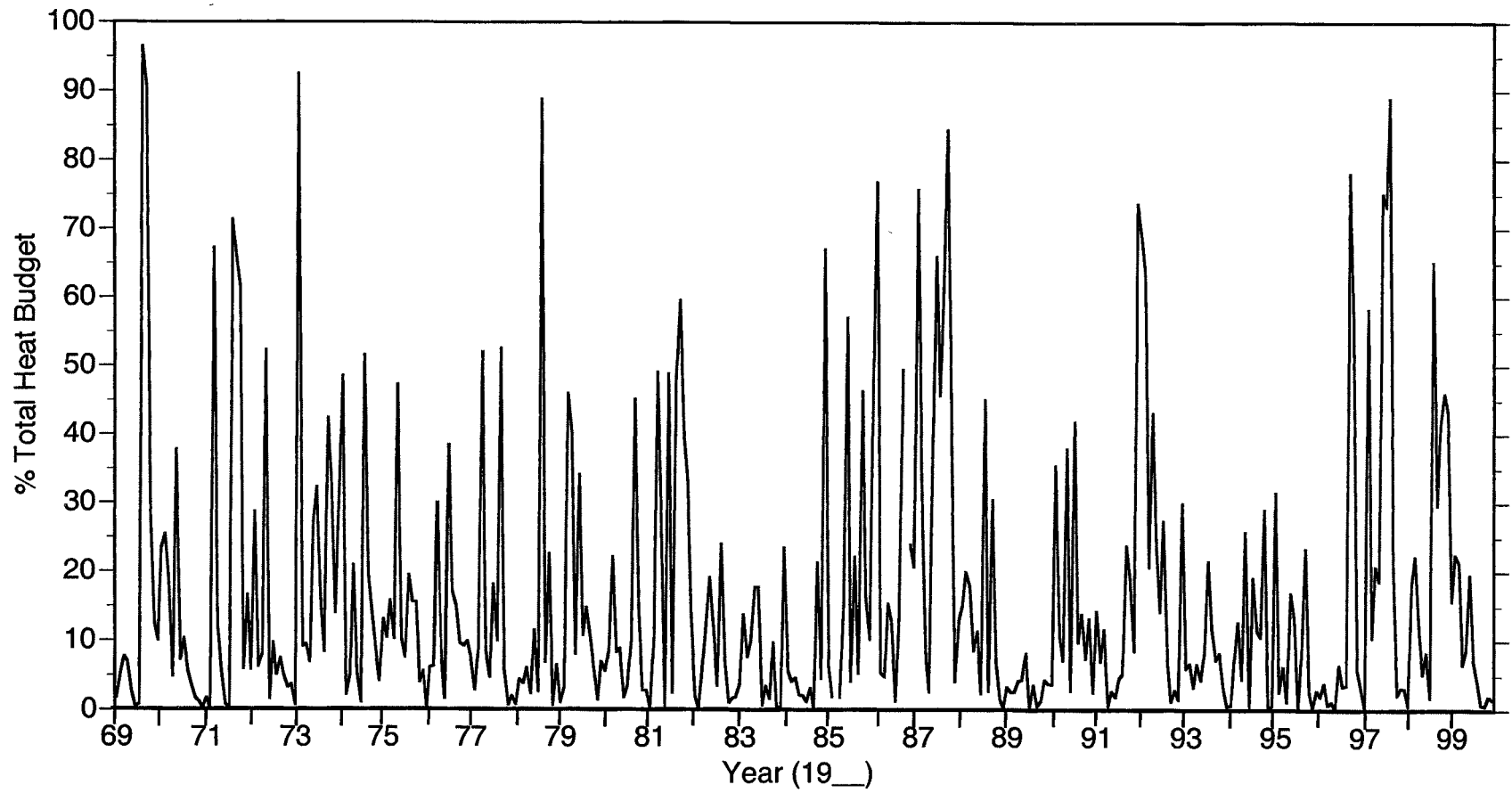


Figure 6. Percent contribution by month of advection to the net heat budget of Canyon Reservoir.

large volumes of water entering the reservoir will alter the relative contribution of advected heat.

Surface heat inputs

Net short wave solar radiation (that reaching the water's surface) accounted for $37.1 \pm 0.4\%$ (mean \pm 95% confidence limit for the 31 yr of monthly data) of the heat entering the reservoir's surface. There is an obvious and expected annual pattern in direct solar heat input (Figure 7, Hostetler 1995), as the amount of short wave solar radiation striking any point on earth is controlled by the solar angle and the distance between the earth and sun. J_{sn} is further reduced by scattering as well as the attenuation of short wave radiation by atmospheric moisture and cloud cover (Allen et al. 1998). For this study area, J_{sn} reaches its peak in July (study period mean = $565 \text{ cal cm}^{-2} \text{ d}^{-1}$) and its minimum in December (study period mean = $251 \text{ cal cm}^{-2} \text{ d}^{-1}$). Coefficients of variation for net solar radiation were always low but highest for November-February (C.V. 9–11%) and lowest during June-August (C. V. 6-8%). The coefficients of variation correspond to the times of the year with the greatest (November-February) and lowest (June-August) amounts of cloud cover. The variability of J_{sn} in this study

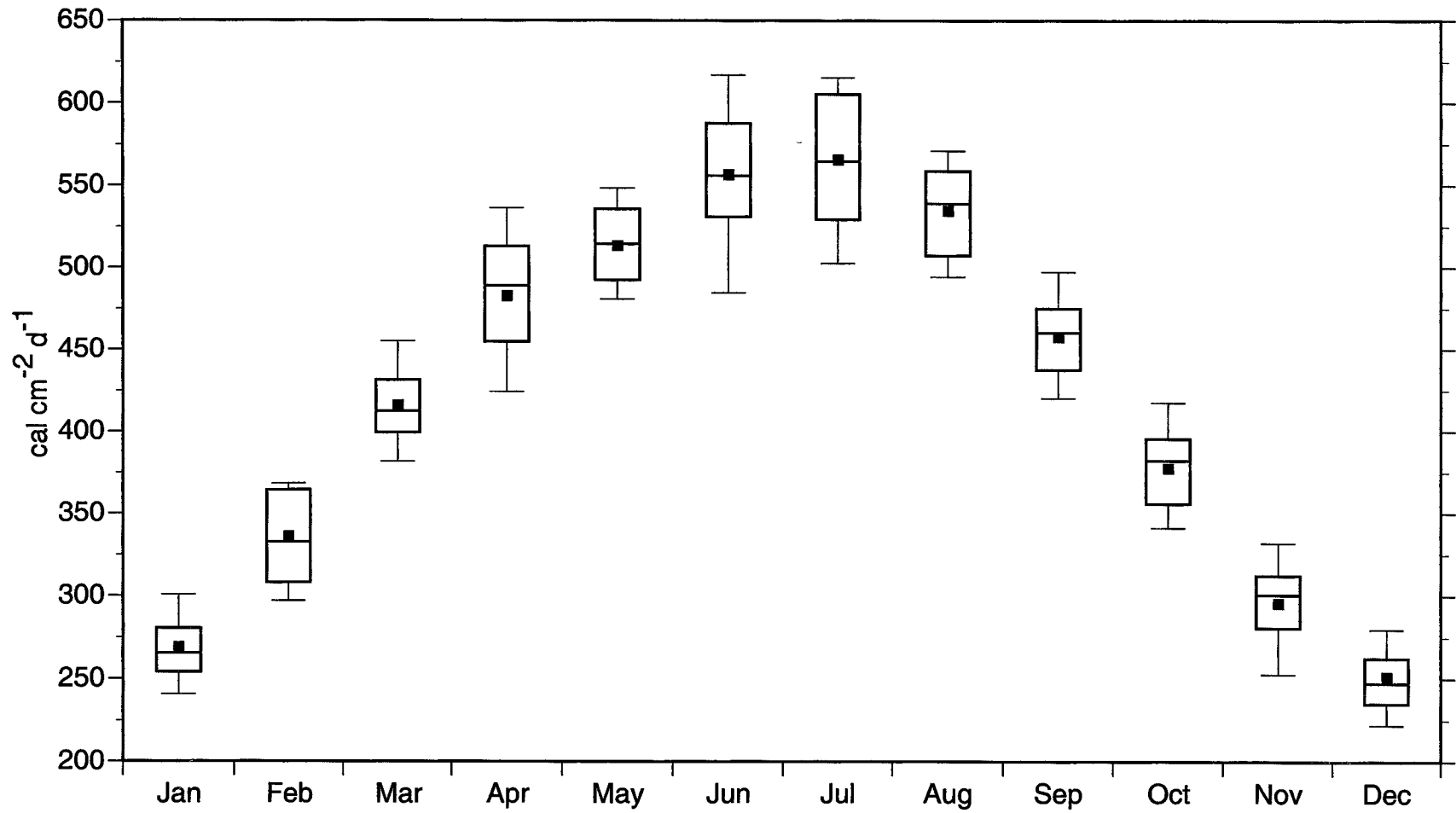


Figure 7. Mean monthly amount and variability of heat gain through net solar radiation 1969-1999.

was considerably less than that reported by Townsend et al. (1997) for two tropical Australian reservoirs (7-29%).

Long wave radiation (J_{an}) accounted for the majority of the surface heat input into the reservoir ($62.9 \pm 0.4\%$). This form of radiation is dependent on atmospheric temperature and humidity, and reaches its maximum in July and minimum in January (Figure 8). Variability within each month ranged between 1 and 4%, similar to the 1-2% reported by Townsend et al. (1997) for their study of two tropical Australian reservoirs.

Over this study period surface heat input to Canyon Reservoir had a mean total monthly gain of $1116 \text{ cal cm}^{-2} \text{ d}^{-1}$, and intra-annual fluctuation was on the order of $700 \text{ cal cm}^{-2} \text{ d}^{-1}$. No surface heat input trends were evident over the study period of the reservoir. Figure 9 shows the monthly contributions of both J_{sn} and J_{an} to the surface of Canyon Reservoir during this study.

Short wave solar radiation was calculated for the last 9 yr of this study. A comparison of measured to calculated values was possible for only one year, and the calculated values slightly overestimated December-February values (1-4%) and underestimated June-August values (1-20%). As mentioned earlier, the atmospheric attenuation coefficient used to calculate long wave radiation input

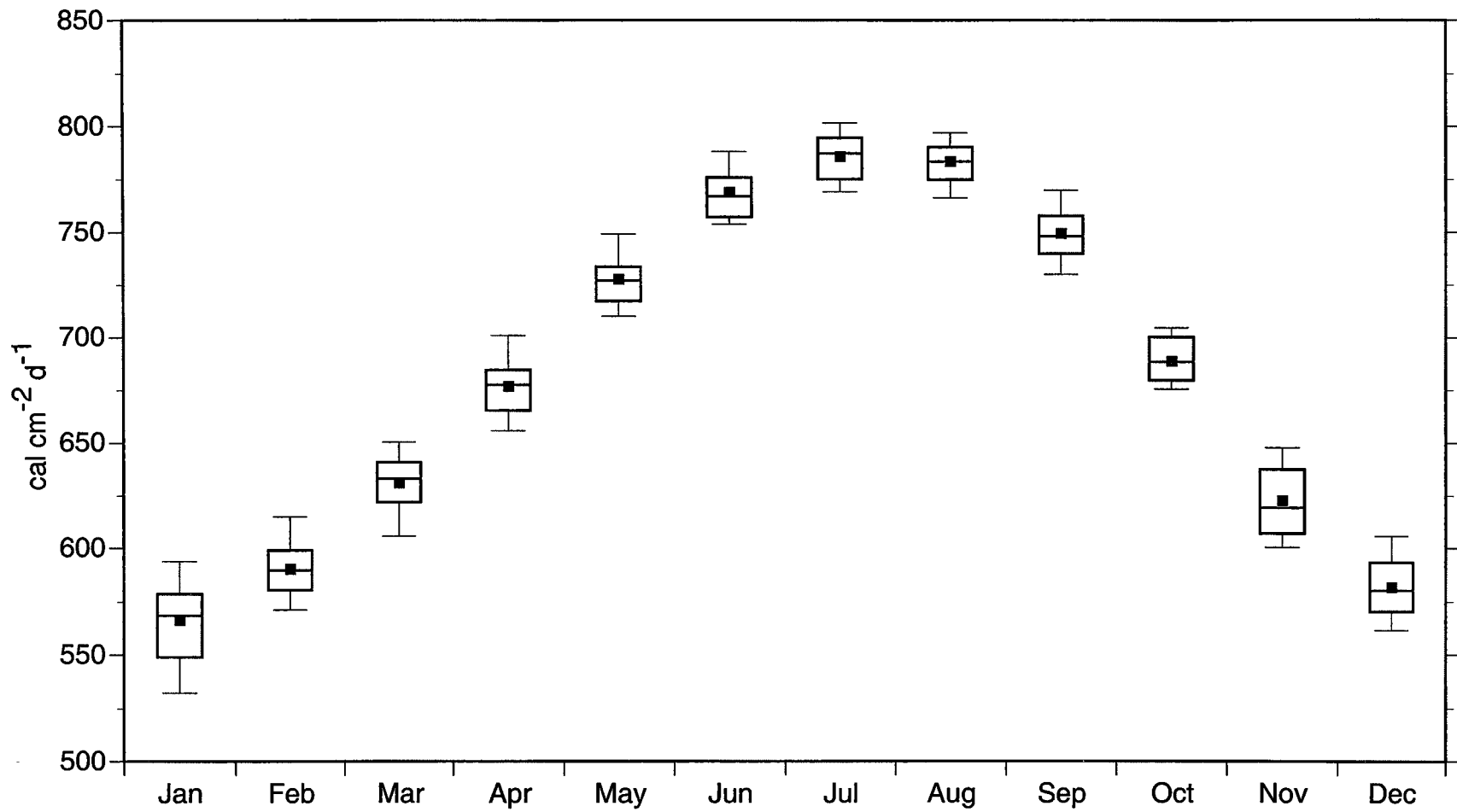


Figure 8. Mean monthly amount and variability of heat gain through atmospheric long wave radiation 1969-1999.

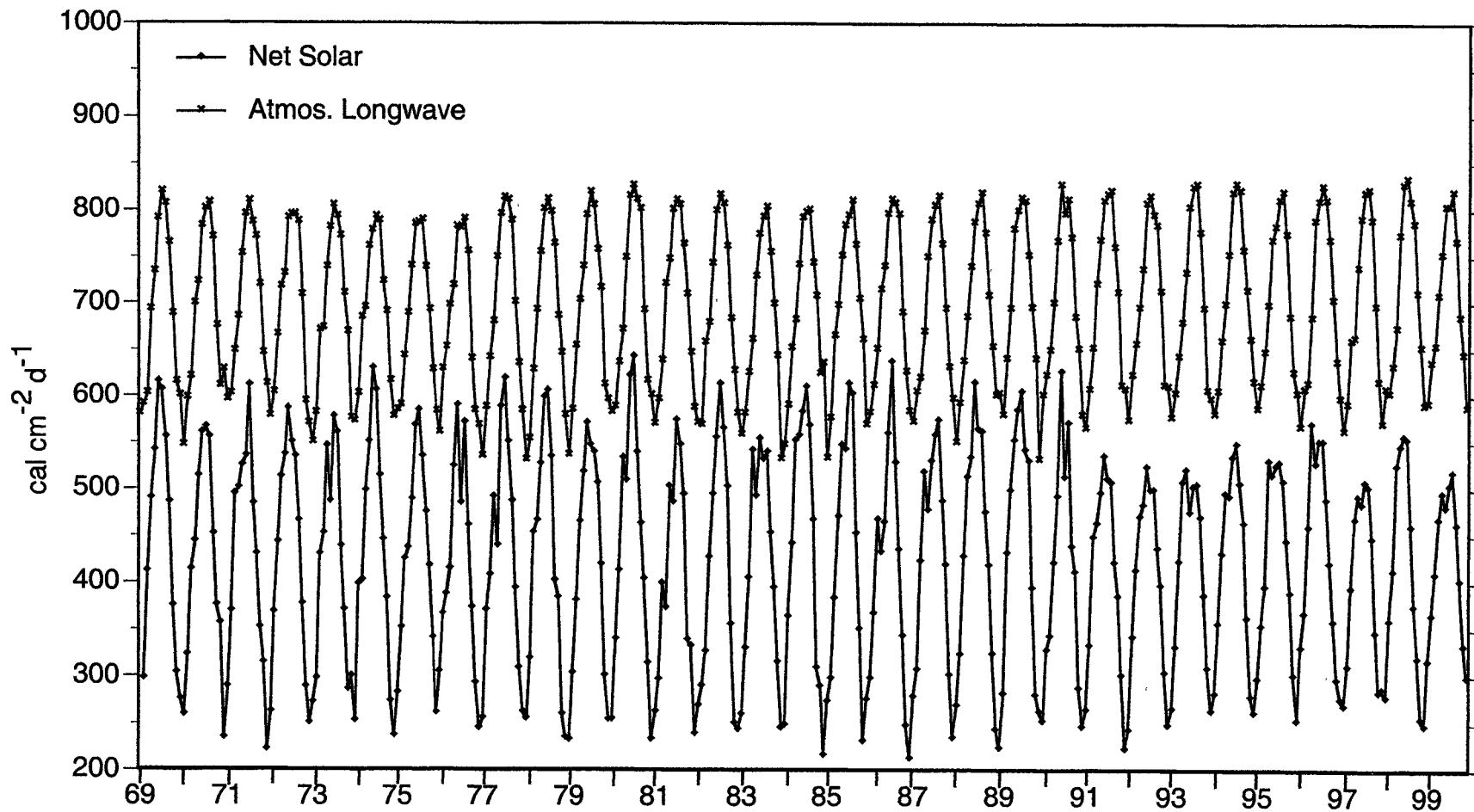


Figure 9. Net solar and atmospheric long wave radiation heat input in Canyon Reservoir 1969-1999.

was derived using local climatic conditions (see Appendix D). The calculated values of the atmospheric attenuation coefficient (A) were higher than the maximum value listed by Chapra (1997) and on the upper end of the range obtained by Koberg (1964). Chapra (1997) did not provide any insight for specifying a value for this coefficient.

Surface heat losses

Long wave back radiation (J_{br}) was the predominant means of heat removal from the reservoir. Because long wave radiation is a function of temperature, seasonal variation in J_{br} heat loss was similar to that of atmospheric long wave heat input (Figure 10). Long wave back radiation accounted for the majority of total surface heat loss ($76.8 \pm 0.6\%$).

Evaporative heat loss (J_e) was the most variable of the surface heat flux terms (C.V. range of 18-50%) because it is dependent on wind speed and vapor pressure gradients. Since temperature changes are more incremental than shifts in wind speed, fluctuations on daily, monthly and seasonal scales would be expected. J_e accounted for $20.8 \pm 0.6\%$ of the monthly total heat lost from the surface of the reservoir. The amount and patterns of variability in evaporative

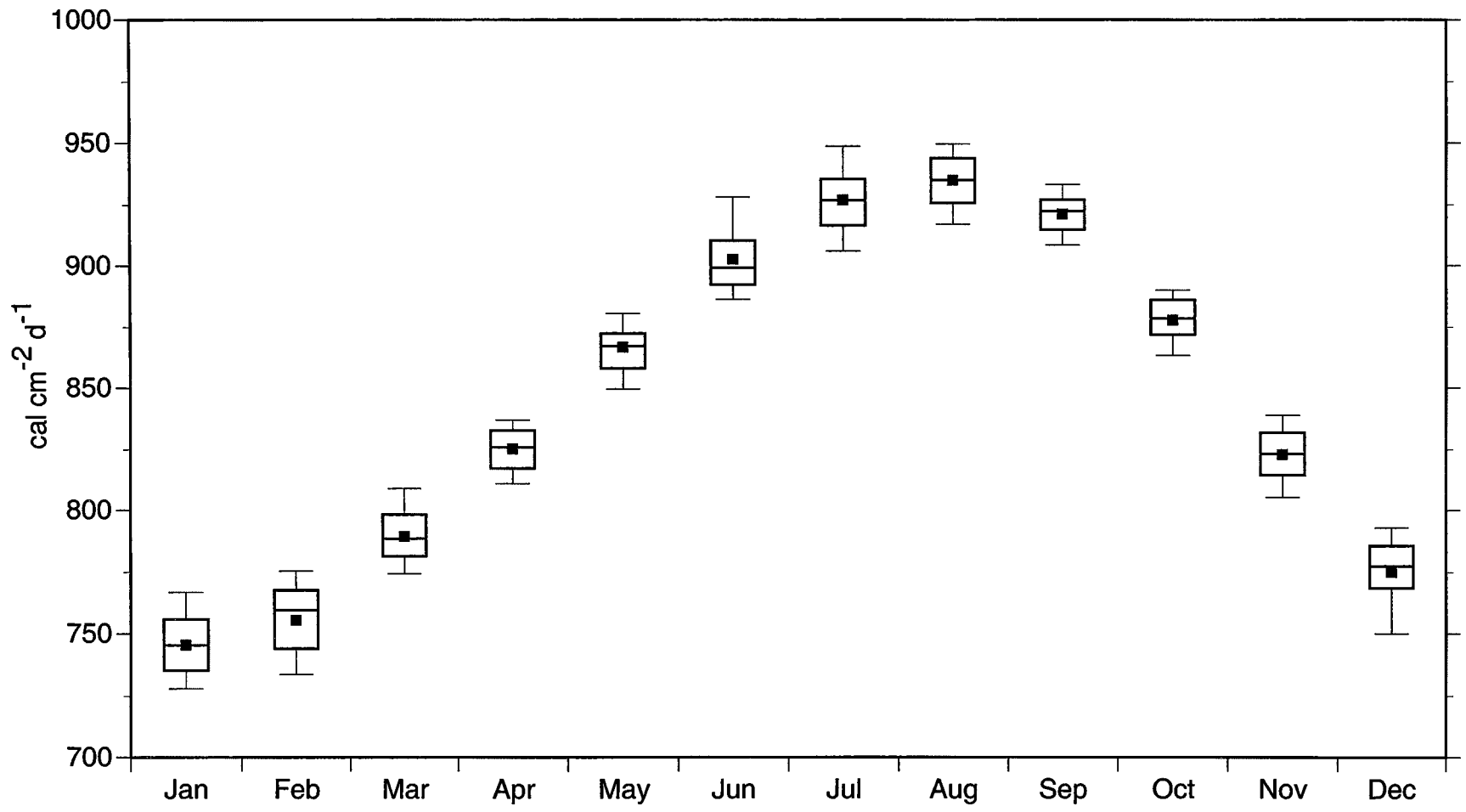


Figure 10. Mean monthly amount and variability of heat loss through water long wave back radiation 1969-1999.

heat loss generally follow that of solar radiation, that is, lowest values in winters (December-February) and highest values in summers (June-August) (Figure 11).

Heat loss attributed to conduction and convection (J_c) in Canyon Reservoir was comparatively small. The rate of conductive heat loss is a function of the temperature gradient between water and air and wind speed, so one would expect the greatest transfer when ambient air and water temperatures are largest (Figure 12). Between December and February the reservoir lost heat to the surrounding environment, and absorbed heat during the summer months (June-August). Conduction and convection accounted for $2.4 \pm 0.2\%$ of the total heat loss from the surface of the reservoir, but this is misleading in that during June through August, this surface heat flux component acts as a heat source for the reservoir.

Figure 13 details the three components of surface heat loss from the reservoir over the study period. Over this 31-yr period, the surface of Canyon Reservoir has lost a monthly mean of $1087 \text{ cal cm}^{-2} \text{ d}^{-1}$. Heat lost through water long wave back radiation was approximately four times that of evaporation, while conduction contributed relatively little to overall heat flux (Figure 13).

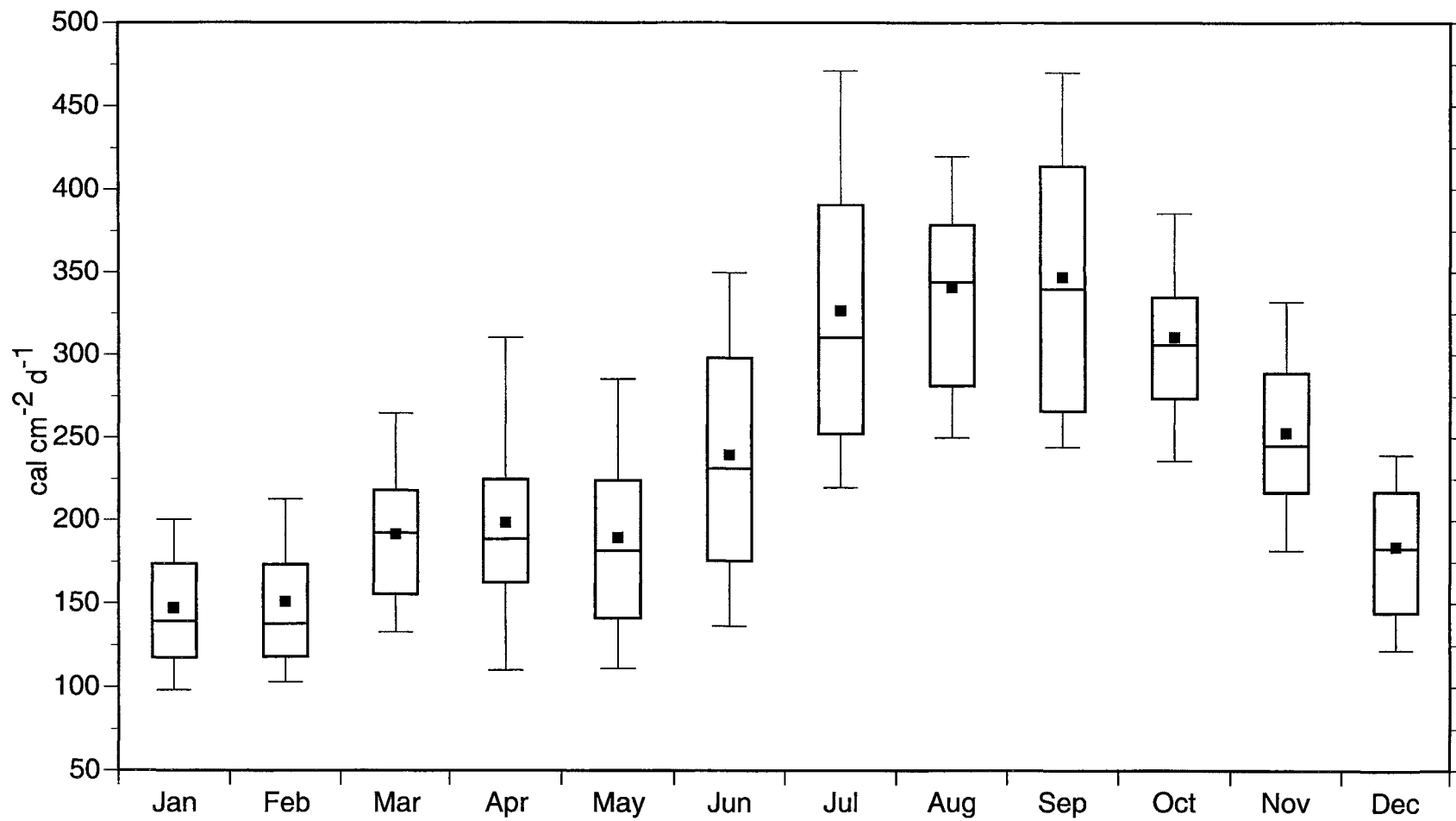


Figure 11. Mean monthly amount and variability of heat loss through evaporation 1969-1999.

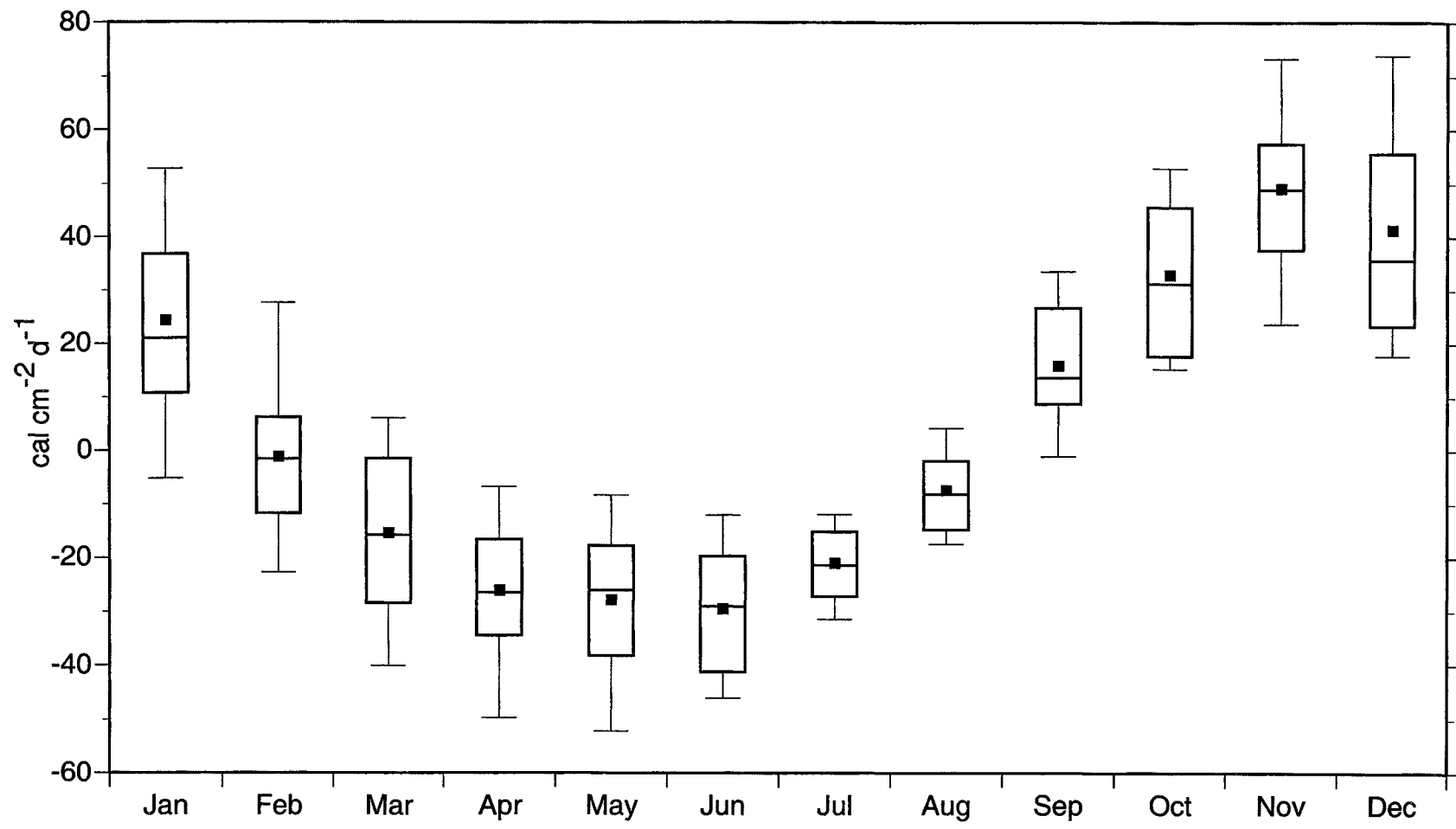


Figure 12. Mean monthly amount and variability of heat loss through conduction 1969-1999.

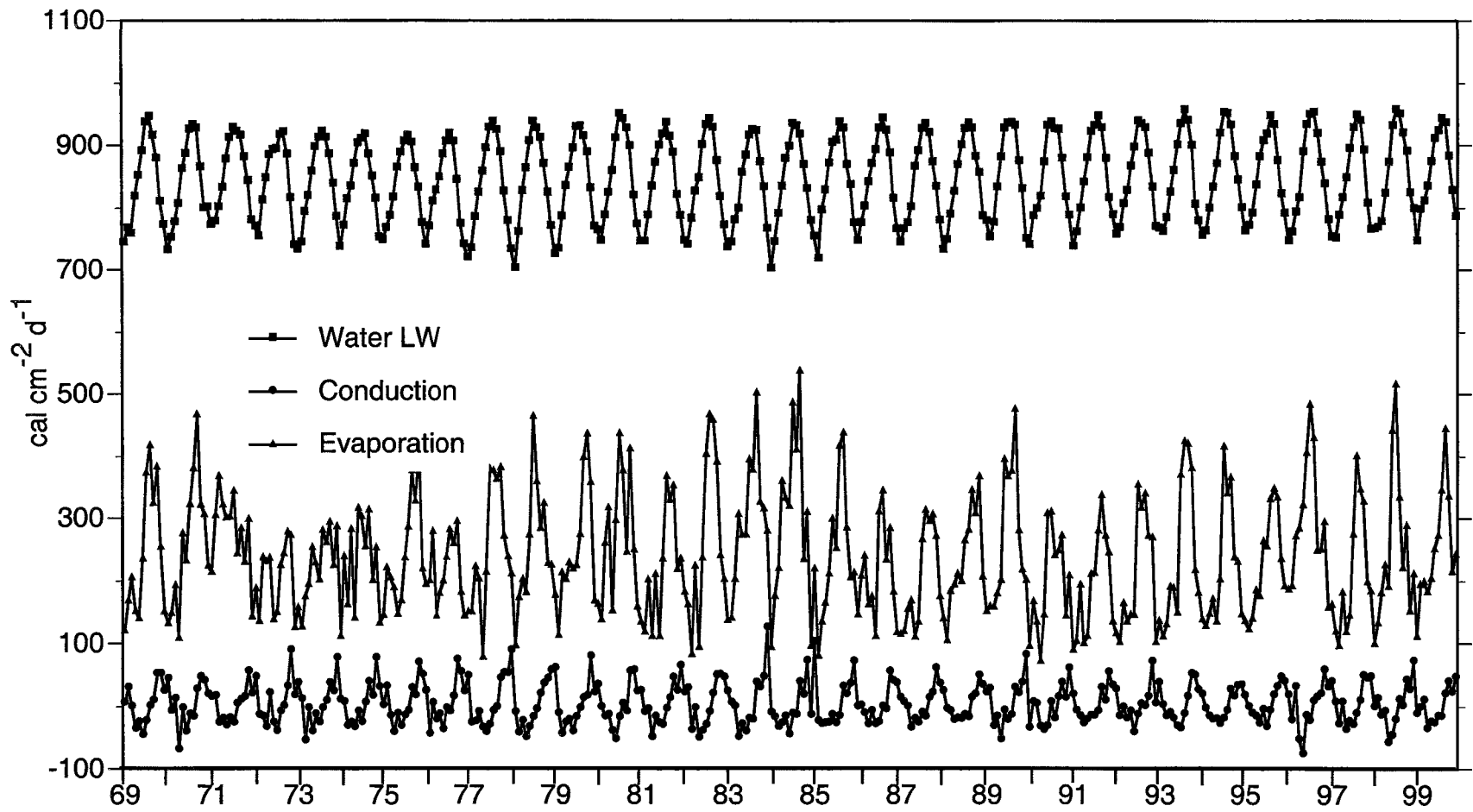


Figure 13. Heat loss due to conduction, evaporation and water long wave back radiation in Canyon Reservoir 1969-1999.

Net surface heat flux

The five components of surface heat flux are combined in Figure 14. Over an annual cycle, heat transfer rates at the surface of the reservoir can change as much as $700 \text{ cal cm}^{-2} \text{ d}^{-1}$, and over this study period, the reservoir gained approximately $29 \text{ cal cm}^{-2} \text{ d}^{-1}$ more than it lost through surface heat exchange. The pattern of surface heat input was regular and fairly uniform over the study period. This is not surprising because the source of these inputs is solar radiation, so any large shifts in heat input would be unlikely. Heat loss, however, does not follow such a uniform pattern due to the variability in the evaporative heat loss component of surface heat flux.

Net heat budget

The net heat balance for Canyon during this period is presented in Figure 15, and the repeating annual pattern of net heat is apparent. Canyon Reservoir appears to remove a mean of approximately $44 \text{ cal cm}^{-2} \text{ d}^{-1}$ (approximately 4% of the total average monthly heat input) from its surrounding environment each month.

Wetzel and Likens (1991) have stated that there should be no net heat transfer over the annual cycle of a lake. Since Canyon Reservoir apparently

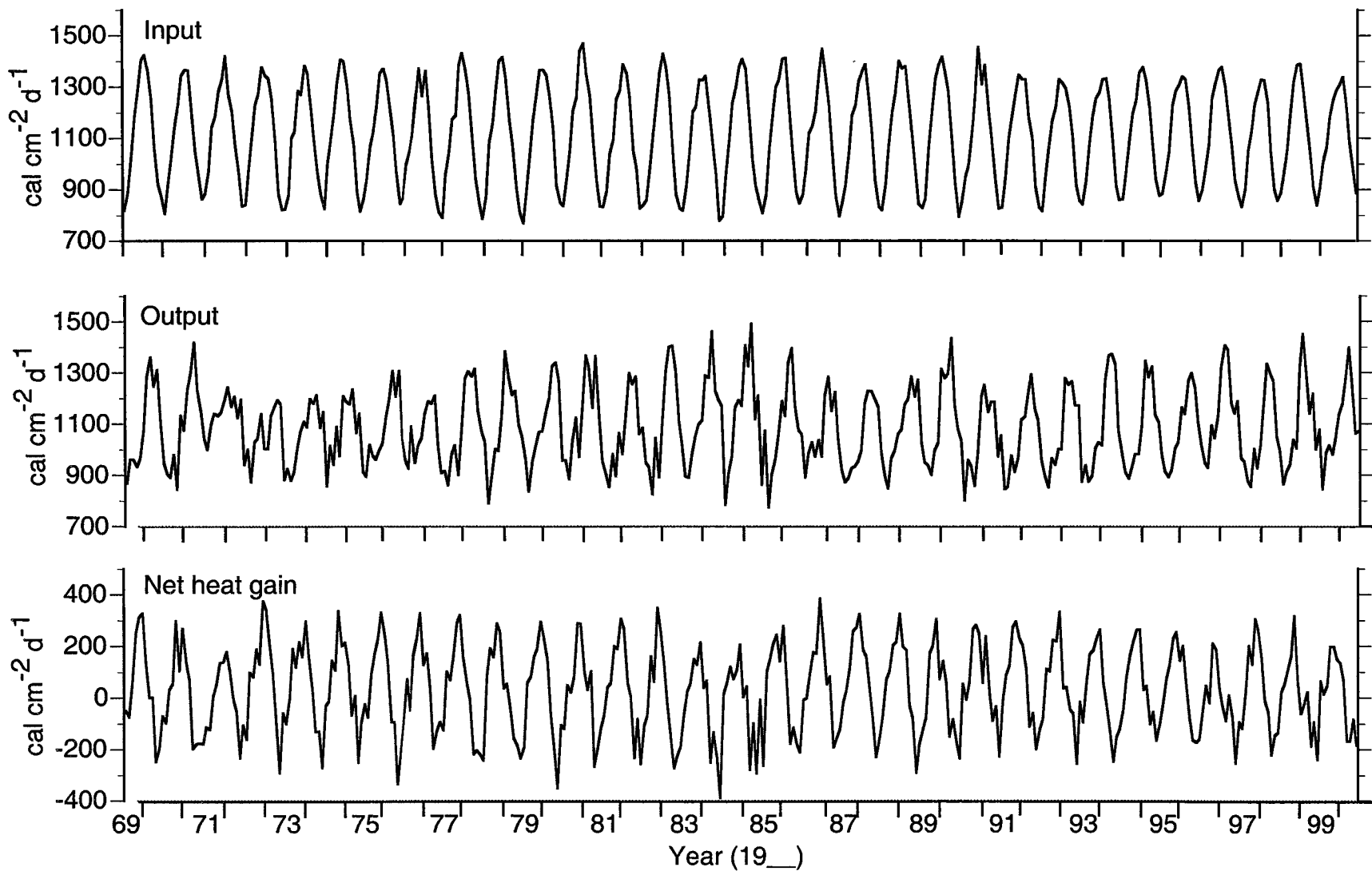


Figure 14. Heat input, output and net gain for the surface flux components of the heat budget of Canyon Reservoir.

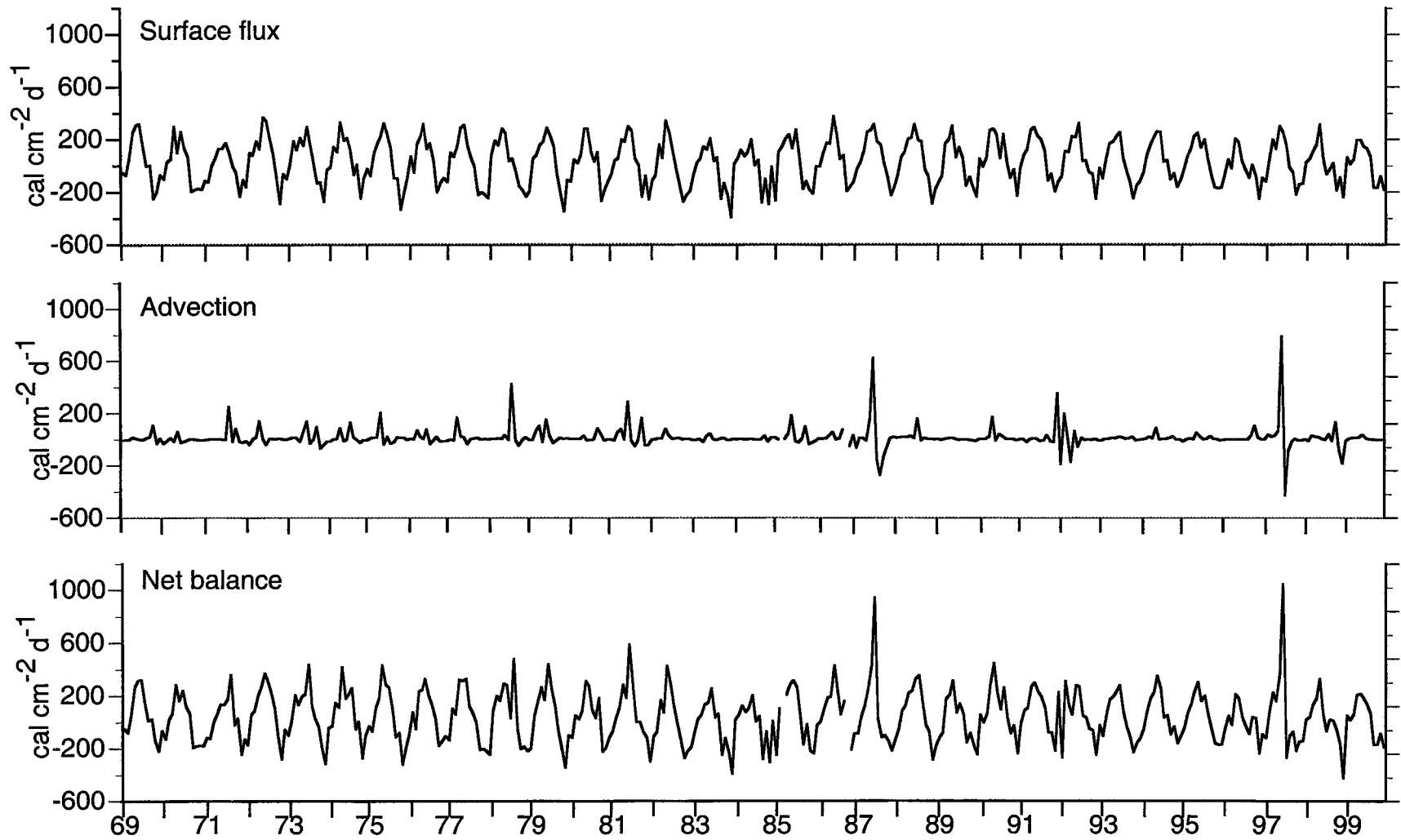


Figure 15. Monthly heat gain through surface flux, advection and net balance in Canyon Reservoir 1969-1999.

gains heat and it does not appear to be warming, the reservoir violates the first law of thermodynamics. Because the first law requires heat balance, the surplus heat content of the reservoir must be a result of the cumulative errors in the many equations used to provide data for the construction of the heat budget.

Figure 16 presents a generalized annual heat budget for Canyon Reservoir. This figure was compiled from grand annual means for each component of the heat budget over the 31-yr period, but there is great variability within some of the components. Advection accounts for 33% (or 5.02×10^{12} cal) of the total heat flux through the reservoir for the “typical” year. Surface heat flux accounts for the remaining 67% (1.02×10^{13} cal), producing an annual net heat balance of 1.52×10^{13} calories. Overall, the reservoir receives a mean annual heat load of 3.91×10^{14} calories and removes approximately 96% (3.76×10^{14} cal) of that load.

A heat budget for the average annual cycle showing the monthly contributions of each component is presented in Figure 17. The general patterns seen in Canyon Reservoir were also observed by Dutton and Bryson (1962) in a shallow temperate lake; that is, a sinusoid pattern of net heat gain, positive in the summer months (June-August) and negative in the winter months (December-

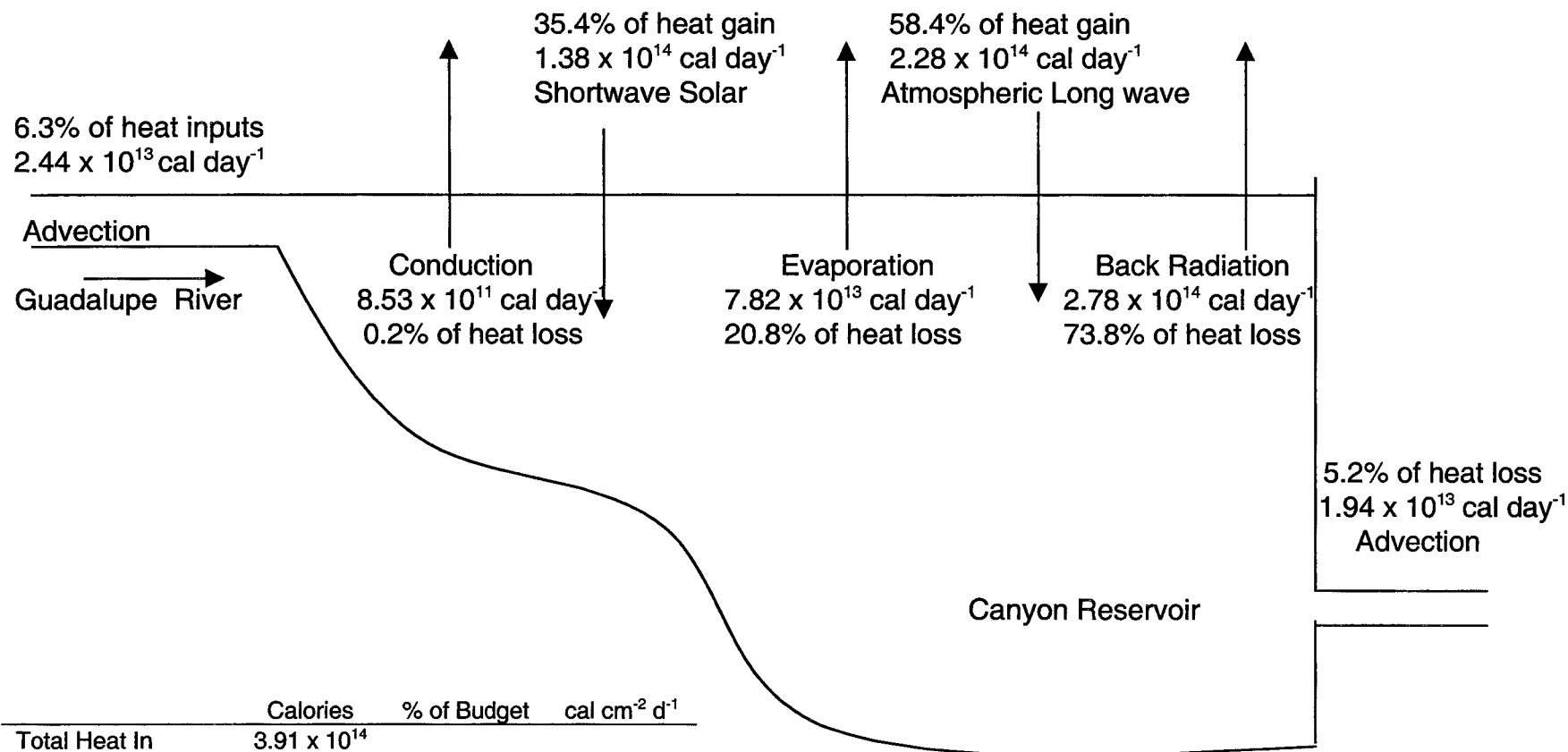


Figure 16. Generalized annual heat budget for Canyon Reservoir.

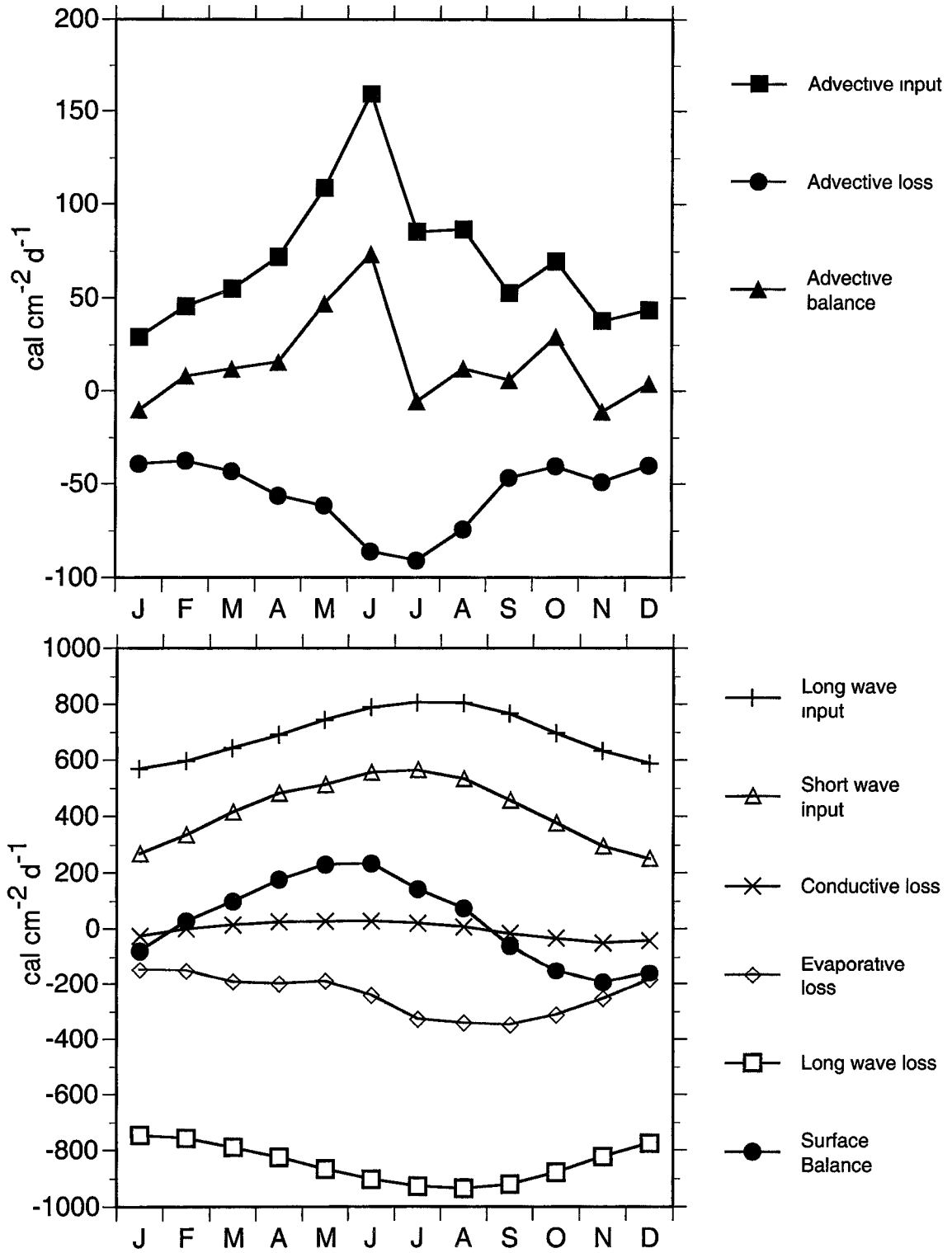


Figure 17. Generalized monthly heat budgets for the advective and surface flux components of the heat budget of Canyon Reservoir. Data presented are 31-year mean values ($n = 31$).

February). The magnitude of the values for Canyon Reservoir's individual heat balance terms were intermediate between those for lakes in tropical and temperate latitudes, but more closely matched those seen by Townsend et al. (1997) in two tropical Australian reservoirs.

Relative importance of advective heat

The magnitude of advective heat gain is less than that of the surface most of the time, but its importance to the overall heat budget is its timing. As shown in Figure 17, surface heat flux oscillates between positive and negative over the annual cycle. Because of this cycling, surface heat flux approaches zero twice each year - February and November. The closer the net surface heat balance is to zero, the larger the proportion of the total heat balance advective heat contributes. Townsend et al. (1997) saw similar shifts in surface and advective dominance during wet and dry seasons in the heat budgets of tropical Australian reservoirs.

Floods have large impacts on the heat budgets of reservoirs. Again, the timing of the event is important in determining its impact. Spring (March-May) and autumn (September-November) floods would be expected to have the greatest impact because net surface heat flux is at its lowest. If floods enter the

reservoir in the winter (December-February), however, net heat loss from the reservoir is reduced. At this time of year, surface heat flux is negative (heat is lost to the atmosphere) and storm waters are generally warmer than the reservoir. If the volume of this warmer inflowing water is sufficiently large, the contribution of surface heat losses to the heat budget will be reduced compared to that of the incoming water.

This was the case during 1991-1992 when a December flood disrupted the regular cycle of heat dynamics in the reservoir (Figure 18). Prior to the flood, heat transfer into the reservoir was almost entirely the result of surface heat flux. This is seen in the figure as, during the first 10 months of 1991, surface heat flux and net heat gain values were virtually the same. When flood water entered the reservoir, the net heat gain patterns switched to almost exactly follow those of advection, resulting in the reversal of the expected seasonal pattern of heat loss. After the flood volume passed through the reservoir, surface heat flux again dominated the heat budget. Heat carried in during floods in the warmer months had additive effects on reservoir heat gain, as can be seen in Figure 15 for the years of 1987 and 1997. In the case of 1997, reservoir surface temperature was

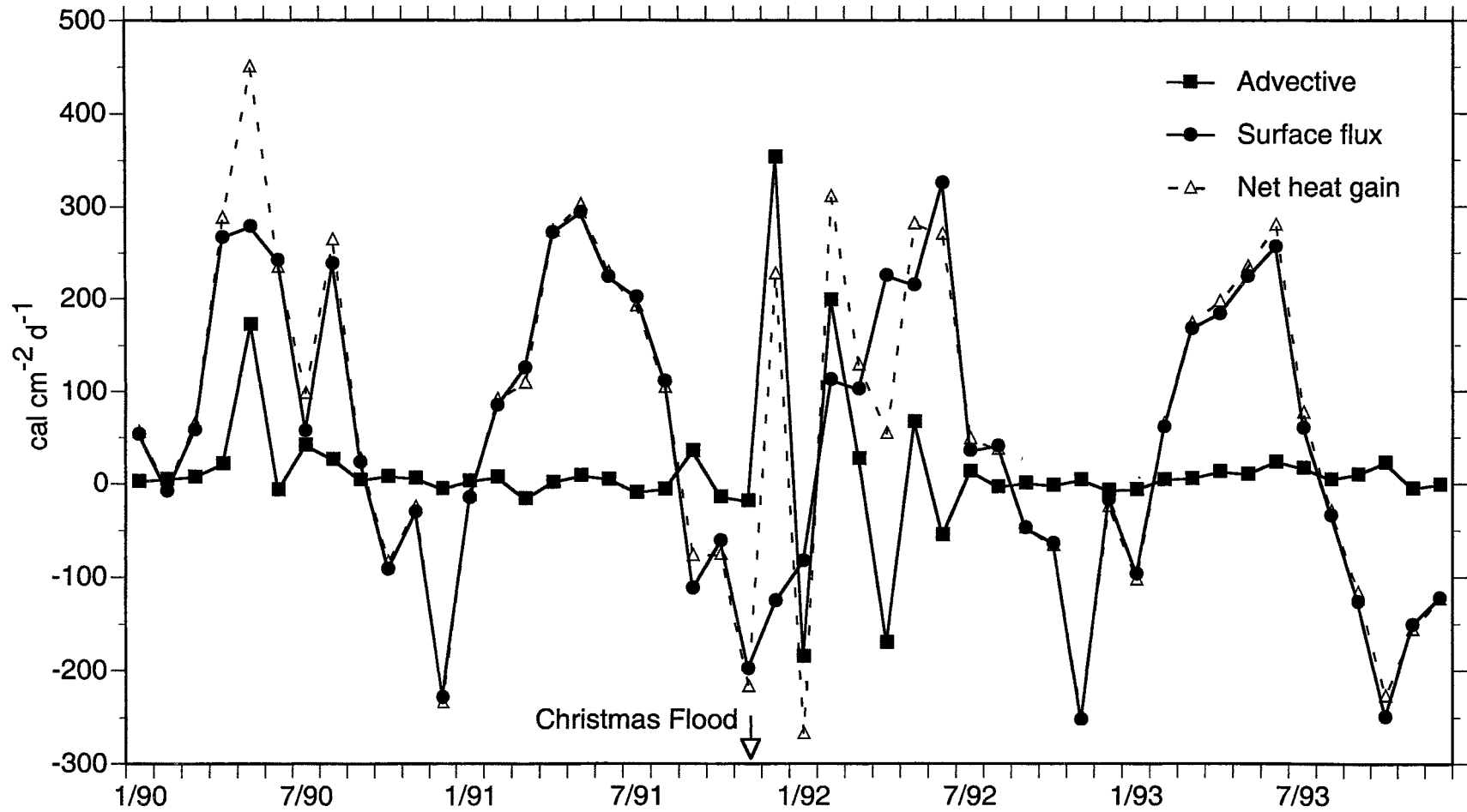


Figure 18. Monthly heat gain through surface flux, advection, and net balance 1990 - 1993.

warmer than the inflowing waters, but the volume of the flood still carried in enough heat to substantially affect the budget.

Heat budgets in wet vs dry years

To further explore the role advection plays in the heat dynamics of Canyon Reservoir, data from the three wettest (1987, 1992 and 1997) and three driest (1983, 1984 and 1989) years were compared to the annual means for each component of the heat budget. The classification of each year as wet or dry was based on water quantity entering the reservoir for the year. Differences in heat exchange by J_{sn} , J_{an} , J_{br} and J_c were minimal and therefore did not contribute greatly to the differences observed between wet and dry years. This comparison did, however, show marked differences with respect to advective heat, evaporative heat loss and net heat gain (Table 3).

The amount of advected heat moved into the reservoir in the wettest years was nine times greater than that in dry ones, but the net heat gain was only three times greater. The discrepancy between the amount of heat advected into the reservoir versus heat retained was due to the reservoir management practices. In dry years evaporation was 19% greater than the 31-yr mean rate, while the wettest years had evaporation rates of only 81% of the 31-yr mean annual rate,

most likely due to the differences in air vapor pressure (humidity) during the wetter years.

Net heat balances in Canyon Reservoir were quite different between the wet and dry years. In the driest years, the reservoir showed net heat loss due to increased evaporative losses (45 cal cm⁻² d⁻¹ more than the 31-yr mean) and decreased heat input through advection (four times less than the 31-yr mean). The increased heat gain (18 cal cm⁻² d⁻¹) during the wettest years is attributable to the decrease in evaporative losses and solar input.

Table 3. Comparison of the individual heat budget component's 31-year means to the three driest and three wettest years in Canyon Lake's history.

Heat budget component (cal cm ⁻² d ⁻¹)	31-year mean	Mean for 3 driest years	Mean for 3 wettest years
Heat gain through advection			
In	70.94	18.97	173.52
Out	-55.41	-14.99	-160.71
Net balance	15.53	3.98	12.81
Heat gain through surface flux			
Net short wave solar radiation	420.95	429.29	409.71
Atmospheric long wave radiation	694.93	688.50	695.25
Water long wave back radiation	-844.91	-841.81	-844.81
Evaporation	-239.18	-284.56	-206.44
Conduction	-2.79	-2.76	-3.48
Net balance	29.00	-11.34	50.23
Total heat balance	44.53	-7.36	63.04

Summary

1. The heat budget of Canyon Reservoir is dominated by net radiation ($J_{sn} + J_{an} - J_{br}$) and evaporation.
2. Heat flux in subtropical Canyon Reservoir was intermediate between the tropical reservoirs of Townsend et al. (1997) and the temperate lake examined by Dutton and Bryson (1962).
3. The importance of advective heat gain changes according to time of year and flow regime.
4. The timing and magnitude of floods determine the relative contribution advection makes to heat gain, and these short-term contributions have a major impact on the annual heat budget.
5. There are large differences in reservoir heat budgets between wet and dry years.

APPENDIX A

CONVERSION FACTORS AND SYMBOLS USED

ϵ	Emmissivity of a radiating body (0.03)
ϕ	Latitude (rad)
δ	Solar declination (degrees)
ω_s	Sunset hour angle (degrees)
A	Atmospheric attenuation coefficient (dimensionless)
C_1	Bowen's constant (0.47 mm Hg °C ⁻¹)
cal cm ⁻² d ⁻¹	Equivalent to 0.484 W m ⁻² or 0.00419 MJ m ⁻² d ⁻¹
C_p	Specific heat of water (cal g ⁻¹ °C ⁻¹)
d_r	Inverse relative distance between the earth and sun
e_{air}	Vapor pressure of air (mm Hg)
e_s	Saturation vapor pressure (mm Hg)
$f(U_w)$	Function describing wind speed measured at 7m
G_{sc}	Solar constant (0.0820 MJ m ⁻² d ⁻¹)

J	Julian day
J_{an}	Atmospheric long-wave radiation ($\text{cal cm}^{-2} \text{d}^{-1}$)
J_{br}	Water long-wave radiation ($\text{cal cm}^{-2} \text{d}^{-1}$)
J_c	Heat loss through conduction and convection ($\text{cal cm}^{-2} \text{d}^{-1}$)
J_e	Evaporative heat loss ($\text{cal cm}^{-2} \text{d}^{-1}$)
J_{net}	Net heat gain ($\text{cal cm}^{-2} \text{d}^{-1}$)
J_{sn}	Net solar radiation ($\text{cal cm}^{-2} \text{d}^{-1}$)
K_{rs}	Adjustment coefficient for weather pattern influences
$\text{MJ m}^{-2} \text{d}^{-1}$	Equivalent to $23.9 \text{ cal cm}^{-2} \text{d}^{-1}$ or 11.6 W m^{-2}
Q_{in}	Flow into reservoir ($\text{m}^3 \text{s}^{-1}$)
Q_{out}	Flow out of reservoir ($\text{m}^3 \text{s}^{-1}$)
R_a	Extra-terrestrial radiation ($\text{MJ m}^{-2} \text{d}^{-1}$)
R_L	Reflection coefficient (dimensionless)
R_s	Relative solar radiation ($\text{MJ m}^{-2} \text{d}^{-1}$)
R_{so}	Clear sky solar radiation ($\text{MJ m}^{-2} \text{d}^{-1}$)
$SA30\text{day}_{Temp}$	Mean air temperature at San Antonio over previous 30 days ($^{\circ}\text{C}$)
T_{3m}	Reservoir water temperature at 3 m ($^{\circ}\text{C}$)
T_{air}	Air temperature ($^{\circ}\text{C}$)

T_b	Air temperature at Boerne (°C)
T_{in}	Temperature of inflowing water (°C)
T_{max}	Maximum daily air temperature (°C)
T_{min}	Minimum daily air temperature (°C)
T_{out}	Temperature of outflowing water (°C)
T_s	Air temperature at water's surface (°C)
T_{sb}	Water temperature at Spring Branch, Texas (°C)
$W \text{ m}^{-2}$	Equivalent to $0.0864 \text{ MJ m}^{-2} \text{ d}^{-1}$ or $2.06 \text{ cal cm}^{-2} \text{ d}^{-1}$
z	Altitude (m)
π	pi (3.1415.....)
ρ	Density of water (kg m^{-3})
σ	Stefan-Boltzman constant ($11.7 \times 10^{-8} \text{ cal cm}^{-2} \text{ d}^{-1} \text{ }^\circ\text{K}^{-1}$)

APPENDIX B

SOLAR RADIATION CALCULATION

Monthly net solar radiation for 1991-1999 was calculated using methods found in Allen et al. (1998). This procedure involves calculating the total amount of extra-terrestrial radiation reaching the earth. The definition of extra-terrestrial radiation is standardized to mean the amount of radiation reaching the top of the earth's atmosphere as measured on a horizontal surface.

There are three components that affect the amount of extra-terrestrial radiation reaching a given point on the earth: latitude, time of day and day of the year. When the earth tilts on its axis as the year progresses, the amount of radiation received on this horizontal surface changes. The same is true on a daily time-scale as well. Latitude affects the sun's angle to the horizontal. The formula for calculating extra-terrestrial radiation in Allen et al. (1998) is:

$$R_a = \frac{1440}{\pi} G_{scd} [\omega_s \sin(\varphi) \sin(\delta) + \cos(\varphi) \cos(\delta) \sin(\omega_s)] \quad (12)$$

where R_a = extra-terrestrial radiation ($\text{MJ m}^{-2}\text{d}^{-1}$),

G_{sc} = solar constant ($0.0820 \text{ MJ m}^{-2}\text{d}^{-1}$),

d_r = inverse relative distance between earth and sun (see equation 13),

ω_s = sunset hour angle (see equation 14),

ϕ = latitude in radians, and

δ = solar declination (see equation 15).

$$d_r = 1 + 0.033 \cos\left(\frac{2\pi}{365} J\right) \quad (13)$$

where d_r = inverse relative distance between the earth and sun, and

J = julian day of the year.

$$\omega_s = \arccos[-\tan(\phi)\tan(\delta)] \quad (14)$$

$$\delta = 0.409 \sin\left(\left(\frac{2\pi}{365} J\right) - 1.39\right) \quad (15)$$

Once R_a has been determined, the net solar radiation reaching the ground (R_s) must be calculated. Allen et al. (1998) offer the following formula to take into account factors attenuating solar radiation (cloud cover). Their equation is based on the assumption that diurnal temperature differences can be related to cloud cover.

$$R_s = R_a(K_{rs})\sqrt{T_{\max} - T_{\min}} \quad (16)$$

where T_{\max} = maximum air temperature ($^{\circ}\text{C}$),

T_{\min} = minimum air temperature ($^{\circ}\text{C}$), and

K_{rs} = adjustment coefficient (0.16 or 0.19).

The adjustment coefficient is decided based on the location's proximity to large water bodies. The lower value is used when there is less influence on weather patterns by large bodies of water than by land mass. The higher values would be chosen for more coastal areas. In this study, a value of 0.16 for K_{rs} was selected.

APPENDIX C

OUTFLOW TEMPERATURE CALCULATIONS

Outflow temperatures from Canyon Reservoir are affected by several variables including flood management practices, hydrogeneration, water residence times and flow into the reservoir. The combination of these factors makes accurate estimation of outflow temperatures difficult, especially when there are few hydrological data from which to build relationships.

One of the best independent variables for predicting outflow temperatures is discharge from the reservoir, especially when flow into the reservoir is generally constant and the reservoir is stratified. During times when the reservoir is mixed, meteorological variables seem to drive outflow temperatures.

Table 4 presents the equation components for predicting outflow temperatures over the 31-yr study period of Canyon Reservoir. Independent variables used to develop this portion of the model are cumulative annual discharge from the reservoir (\log_{10} of m^3), mean monthly air temperature ($^{\circ}C$),

mean monthly air temperature ($^{\circ}\text{C}$) of the previous December and current January and February, mean monthly air temperature ($^{\circ}\text{C}$) of the previous month, mean air temperature ($^{\circ}\text{C}$) of the previous December and current January, and the coldest mean monthly air temperature ($^{\circ}\text{C}$) of the previous December or the current January. All air temperature data were from Boerne, Texas.

Table 4. Intercepts, slopes and descriptive statistics from the regression equations for predicting outflow temperatures of Canyon Reservoir. A= slope of the coldest mean air temperature of Dec & Jan, B= slope of mean air temperature of Dec & Jan, C= slope of \log_{10} cumulative yearly discharge, D= slope of mean air temperature (Dec, Jan, and Feb), E= slope of mean air temperature for the month, F= slope of the mean air temperature of the previous month.

Month	Intercept	A	B	C	D	E	F	n	r ²
Jan	1.992	0.454	0.602					28	0.769
Feb	-9.861			1.505	1.213	-0.234		25	0.841
Mar	-5.795			1.281	0.741			27	0.703
Apr	-14.917			2.695	0.657			27	0.790
May	-14.756			3.554				11	0.752
Jun	-28.127			5.256				11	0.826
Jul	-38.758			6.618				10	0.817
Aug	-43.110			7.206				10	0.814
Sep	-44.823			7.432				11	0.827
Oct	-44.276			7.409				11	0.829
Nov	-11.031			3.324				11	0.606
Dec	3.596					0.579	0.374	22	0.675

APPENDIX D

ATMOSPHERIC ATTENUATION COEFFICIENT CALCULATION

The choice of the value used for the atmospheric attenuation coefficient (A) used in equation 2 has considerable impact on its result. Varying this coefficient by 0.2 can change the equations results by 20%, and warrants investigation into the rationale for choosing a value. Chapra (1997) recommends a value between 0.5 and 0.7, while Kroberg (1964) reports using values between 0.460 and 0.735. Kroberg (1964) presents a family of curves that relate air temperature and the ratio of clear sky radiation (R_{so}) to net solar radiation (R_s for calculated values or J_{sn} for directly measured values). If these two variables are known, the appropriate value for A can be obtained by extrapolation. R_{so} can be approximated by equations found in Allen et al. (1998). The formula used in this study was

$$R_{so} = (0.75 + 2 \times 10^{-5} z) R_a \quad (17)$$

where z = observation elevation (m asl).

These procedures were used to select a more appropriate value for the atmospheric attenuation coefficient. Values used to calculate atmospheric long wave radiation (equation 2) for each month are listed in Table 5.

Table 5. Atmospheric attenuation coefficients for each month used to calculate atmospheric long wave radiation input into Canyon Reservoir.

Month	Atmospheric attenuation coefficient
Jan	0.705
Feb	0.710
Mar	0.718
Apr	0.717
May	0.720
Jun	0.723
Jul	0.725
Aug	0.725
Sep	0.720
Oct	0.710
Nov	0.715
Dec	0.710

APPENDIX E

SUMMARY STATISTICS FOR THE VARIABLES USED TO DETERMINE THE NET HEAT BUDGET OF CANYON LAKE.

Spring Branch flow ($\text{m}^3 \text{s}^{-1}$)

Statistics	Jan	Feb	Mar	Apr	May	Jun	Jul	Aug	Sep	Oct	Nov	Dec
Mean	10.58	13.89	14.00	14.04	17.96	26.16	12.80	12.67	7.75	12.88	9.07	13.46
n	31	31	30	31	31	31	31	31	31	30	31	31
σ	11.17	28.16	18.31	15.64	15.50	44.29	17.09	25.97	6.04	13.13	6.51	24.86
C.V.	106	203	131	111	86	169	133	205	78	102	72	185
Minimum	2.40	2.58	2.39	1.64	1.24	0.72	0.25	0.57	0.35	1.75	2.33	2.52
Maximum	53.88	117.90	93.63	68.43	62.72	179.22	74.38	141.01	26.66	44.86	26.58	139.49
Median	7.40	6.73	6.55	7.55	12.07	10.26	6.23	4.03	5.65	6.61	6.32	7.04
25th %tile	4.16	4.38	5.26	5.05	7.39	5.41	2.41	2.56	3.85	4.77	4.48	4.30
75th %tile	10.75	14.03	17.79	15.93	25.08	18.47	19.88	11.08	9.05	15.38	11.69	11.88

Sattler flow ($\text{m}^3 \text{s}^{-1}$)

Statistics	Jan	Feb	Mar	Apr	May	Jun	Jul	Aug	Sep	Oct	Nov	Dec
Mean	14.30	13.24	15.79	16.29	15.89	21.03	21.04	15.66	9.32	9.22	10.95	10.73
n	31	31	31	31	31	31	31	31	31	31	31	31
σ	23.19	24.71	20.64	20.74	14.12	22.18	35.03	23.03	9.10	7.16	10.82	12.25
C.V.	162	187	131	127	89	105	166	147	98	78	99	114
Minimum	2.00	2.02	2.03	1.29	1.34	1.15	0.63	0.99	0.82	1.90	1.87	1.21
Maximum	125.68	59.17	111.82	104.93	65.63	78.81	150.32	109.15	36.97	37.29	42.79	60.03
Median	6.04	7.71	9.25	9.43	13.38	11.71	9.04	4.99	6.53	5.09	5.89	5.08
25th %tile	3.72	4.21	4.73	5.59	5.88	7.80	4.05	3.27	3.12	3.35	3.94	3.06
75th %tile	14.84	16.73	19.57	19.03	16.95	21.76	19.76	19.09	11.65	13.99	13.77	14.73

Advective heat input (cal cm⁻² d⁻¹)

Statistics	Jan	Feb	Mar	Apr	May	Jun	Jul	Aug	Sep	Oct	Nov	Dec
Mean	29.08	45.70	56.84	71.95	108.67	159.44	85.27	86.53	52.72	72.00	37.85	43.75
n	31	31	30	31	31	31	31	31	31	30	31	31
σ	27.48	90.31	63.55	75.62	90.16	239.43	102.86	162.45	39.76	72.73	26.41	80.16
C.V.	94	198	112	105	83	150	121	188	75	101	70	183
Minimum	8.70	9.77	10.87	9.57	8.61	5.45	2.06	4.74	2.56	10.30	11.08	5.89
Maximum	131.91	353.22	305.80	342.61	345.63	1005.1	398.11	875.89	170.22	254.64	102.26	452.65
Median	18.56	25.53	32.38	41.24	76.03	70.72	44.69	32.00	40.32	39.18	25.27	24.39
25th %tile	12.39	15.90	23.94	27.44	47.19	37.44	18.66	19.41	25.93	27.17	20.27	14.15
75th %tile	32.90	48.99	68.71	82.52	149.79	126.27	142.59	80.85	62.25	82.99	44.24	37.79

Advective heat loss (cal cm⁻² d⁻¹)

Statistics	Jan	Feb	Mar	Apr	May	Jun	Jul	Aug	Sep	Oct	Nov	Dec
Mean	39.25	37.55	45.58	56.31	61.62	85.96	90.86	74.37	46.74	46.31	48.84	39.95
n	31	31	31	31	31	31	31	31	31	31	31	31
σ	59.16	65.38	53.30	71.45	59.39	95.62	144.62	105.98	48.83	37.33	45.91	44.64
C.V.	151	174	117	127	96	111	159	143	104	81	94	112
Minimum	5.13	4.82	5.26	4.53	4.27	3.74	2.03	3.32	2.80	8.56	9.43	4.84
Maximum	316.90	162.25	279.15	363.87	279.31	375.46	626.48	448.55	221.84	182.93	163.27	221.07
Median	17.36	22.40	29.92	32.88	45.56	45.28	39.62	25.11	30.54	23.64	28.89	19.89
25th %tile	12.12	12.34	15.21	18.78	19.41	29.90	17.96	14.17	13.95	16.00	16.71	12.32
75th %tile	41.67	47.11	56.20	69.79	66.49	90.78	93.34	98.82	62.77	66.98	60.32	47.57

Net solar radiation (cal cm⁻² d⁻¹)

Statistics	Jan	Feb	Mar	Apr	May	Jun	Jul	Aug	Sep	Oct	Nov	Dec
Mean	268.70	335.66	415.67	482.12	512.79	556.38	565.16	534.25	457.29	377.23	295.25	250.91
n	31	31	31	31	31	31	31	31	31	31	31	31
σ	23.70	45.06	33.44	44.64	28.41	44.59	45.05	31.78	31.77	28.05	28.17	21.86
C.V.	9	13	8	9	6	8	8	6	7	7	10	9
Minimum	223.74	282.05	326.67	373.43	438.83	475.09	484.70	459.73	374.39	309.04	231.02	212.83
Maximum	330.73	397.74	494.38	569.69	557.61	629.13	642.33	602.34	530.36	418.63	356.14	299.53
Median	265.38	332.75	412.63	489.23	514.55	556.23	564.76	538.98	460.38	382.39	300.68	247.42
25th %tile	254.36	308.88	400.25	457.59	492.50	532.38	530.42	507.73	438.05	356.75	281.64	235.48
75th %tile	279.67	364.25	431.30	512.79	535.11	587.28	605.39	557.41	474.82	395.16	311.20	262.25

Atmospheric long wave radiation (cal cm⁻² d⁻¹)

Statistics	Jan	Feb	Mar	Apr	May	Jun	Jul	Aug	Sep	Oct	Nov	Dec
Mean	569.50	597.41	644.88	690.67	747.58	796.25	808.73	806.52	767.18	696.81	630.13	588.68
n	31	31	31	31	31	31	31	31	31	31	31	31
σ	20.95	24.71	17.46	16.01	16.48	13.79	13.06	11.20	16.80	15.67	20.35	22.47
C.V.	4	4	3	2	2	2	2	1	2	2	3	4
Minimum	530.63	553.09	602.07	660.78	717.81	774.08	779.73	785.69	722.46	639.33	583.67	532.00
Maximum	607.65	636.03	683.44	720.73	788.66	827.14	833.66	827.48	801.02	718.83	667.68	635.62
Median	572.23	597.22	647.38	692.02	747.30	794.71	810.64	807.09	766.51	696.93	627.33	587.57
25th %tile	554.59	587.91	636.70	679.53	737.77	785.37	799.19	798.67	758.53	688.55	614.96	578.03
75th %tile	582.22	606.30	654.90	698.92	753.57	803.70	817.88	812.98	775.74	708.52	645.38	600.95

Conduction/convection (cal cm⁻² d⁻¹)

Statistics	Jan	Feb	Mar	Apr	May	Jun	Jul	Aug	Sep	Oct	Nov	Dec
Mean	24.21	-1.34	-15.59	-26.21	-27.94	-29.63	-21.20	-7.55	15.79	32.79	48.93	41.22
n	31	31	31	31	31	31	31	31	31	31	31	31
σ	27.31	25.04	18.61	16.01	18.44	12.91	9.53	8.52	12.72	15.84	17.85	26.67
C.V.	113	-5	-119	-61	-66	-44	-45	-113	81	48	36	65
Minimum	-34.89	-44.70	-55.34	-69.61	-76.22	-53.87	-39.84	-22.40	-8.79	8.62	12.92	-14.11
Maximum	102.04	30.75	30.76	6.34	19.91	-5.75	6.39	10.08	38.30	73.70	88.26	125.38
Median	21.03	-1.62	-15.83	-26.52	-26.03	-29.11	-21.35	-8.17	13.69	31.28	48.94	35.66
25th %tile	11.56	-11.25	-28.38	-34.29	-38.05	-41.11	-27.04	-14.77	8.89	17.98	38.48	23.42
75th %tile	36.68	6.19	-1.79	-16.87	-18.27	-19.94	-15.35	-2.55	26.60	45.46	57.16	54.60

Evaporation (cal cm⁻² d⁻¹)

Statistics	Jan	Feb	Mar	Apr	May	Jun	Jul	Aug	Sep	Oct	Nov	Dec
Mean	146.43	150.60	190.75	197.71	188.90	238.95	325.77	339.69	346.17	309.65	252.10	183.39
n	31	31	31	31	31	31	31	31	31	31	31	31
σ	35.84	74.59	56.92	67.91	65.19	84.65	93.80	63.85	87.17	55.75	59.97	48.62
C.V.	24	50	30	34	35	35	29	19	25	18	24	27
Minimum	89.76	79.63	82.31	72.00	78.22	110.49	149.51	223.90	219.87	200.21	143.88	96.24
Maximum	218.10	303.38	367.11	358.59	331.28	440.42	515.49	466.86	536.39	435.09	405.79	286.42
Median	139.13	137.56	192.08	188.45	181.52	230.89	310.17	343.59	339.47	305.57	244.87	182.90
25th %tile	117.95	118.24	156.21	163.00	142.50	183.10	253.13	281.03	271.21	274.68	216.85	145.09
75th %tile	169.58	171.29	216.04	223.79	219.34	297.16	386.59	377.78	408.14	333.89	283.14	215.28

Long wave back radiation (cal cm⁻² d⁻¹)

Statistics	Jan	Feb	Mar	Apr	May	Jun	Jul	Aug	Sep	Oct	Nov	Dec
Mean	745.22	755.24	789.00	824.75	866.23	902.42	926.50	934.47	920.69	877.40	822.43	774.55
n	31	31	31	31	31	31	31	31	31	31	31	31
σ	16.50	23.18	13.54	11.17	10.96	14.18	14.64	11.66	11.18	12.18	15.44	15.27
C.V.	2	3	2	1	1	2	2	1	1	1	2	2
Minimum	701.10	702.24	756.83	797.36	846.15	882.12	893.02	913.81	884.21	843.49	773.31	738.45
Maximum	777.44	796.40	811.90	845.76	888.84	932.07	956.38	954.93	938.80	898.13	854.51	799.56
Median	745.36	759.55	788.58	825.86	867.20	899.12	926.74	934.85	922.20	878.43	823.23	777.43
25th %tile	735.25	744.24	781.88	817.09	858.34	892.82	916.67	925.78	914.68	871.92	814.53	768.57
75th %tile	755.53	767.31	798.21	832.70	872.10	910.04	934.85	943.10	926.79	886.13	831.85	785.20

Spring Branch water temperature (°C)

Statistics	Jan	Feb	Mar	Apr	May	Jun	Jul	Aug	Sep	Oct	Nov	Dec
Mean	11.15	13.22	16.74	20.33	23.82	26.91	28.27	28.23	25.88	21.27	16.03	12.43
n	31	31	30	31	31	31	31	31	31	30	31	31
σ	3.63	14.15	11.97	1.25	1.31	0.94	0.68	0.70	1.09	1.34	2.85	3.12
C.V.	33	107	71	6	6	3	2	2	4	6	18	25
Minimum	7.08	9.05	13.45	18.10	21.84	25.38	25.83	26.14	23.00	16.88	12.74	7.63
Maximum	14.35	16.58	20.22	22.65	26.24	29.27	29.88	29.52	28.16	23.10	19.11	16.38
Median	11.37	13.09	16.81	20.27	23.66	26.84	28.26	28.51	25.88	21.36	16.38	12.64
25th %tile	9.98	12.33	15.99	19.84	23.03	26.14	27.86	27.65	25.43	20.88	14.58	11.73
75th %tile	12.31	13.95	17.64	20.98	24.54	27.55	28.71	28.82	26.59	22.03	17.29	13.27

Outflow temperatures (°C)

Statistics	Jan	Feb	Mar	Apr	May	Jun	Jul	Aug	Sep	Oct	Nov	Dec
Mean	10.97	10.78	11.37	12.94	14.13	15.15	16.25	17.38	17.84	18.49	17.27	14.39
n	31	31	31	31	31	31	31	31	31	31	31	31
σ	1.64	1.74	1.05	1.33	1.35	2.03	2.66	2.62	2.64	2.52	1.08	1.26
C.V.	15	16	9	10	10	13	16	15	15	14	6	9
Minimum	7.62	7.56	8.88	9.87	11.75	11.35	11.25	11.62	11.79	12.83	15.06	11.60
Maximum	14.39	12.90	13.28	16.22	17.55	20.00	21.99	23.12	23.53	23.90	19.57	16.75
Median	11.40	10.77	11.46	13.01	14.28	15.16	16.20	17.06	17.59	18.29	17.24	14.55
25th %tile	10.05	10.07	10.77	12.26	13.42	14.07	14.84	15.64	16.08	16.83	16.44	13.90
75th %tile	11.93	11.74	12.12	13.85	15.05	16.43	17.74	18.82	19.40	20.17	17.97	15.20

Reservoir temperature (°C)

Statistics	Jan	Feb	Mar	Apr	May	Jun	Jul	Aug	Sep	Oct	Nov	Dec
Mean	11.65	12.60	15.75	18.97	22.57	25.61	27.58	28.23	27.11	23.52	18.76	14.41
n	31	31	31	31	31	31	31	31	31	31	31	31
σ	1.58	2.18	1.24	0.99	0.94	1.17	1.19	0.94	0.92	1.03	1.38	1.42
C.V.	14	17	8	5	4	5	4	3	3	4	7	10
Minimum	7.35	7.47	12.77	16.52	20.85	23.92	24.84	26.55	24.10	20.62	14.31	11.01
Maximum	14.69	16.43	17.83	20.81	24.49	28.04	29.98	29.87	28.58	25.26	21.57	16.72
Median	11.68	13.02	15.72	19.07	22.66	25.34	27.61	28.26	27.24	23.61	18.84	14.69
25th %tile	10.71	11.57	15.10	18.29	21.90	24.82	26.79	27.53	26.62	23.06	18.06	13.87
75th %tile	12.64	13.75	16.59	19.67	23.08	26.24	28.26	28.93	27.61	24.26	19.60	15.41

San Antonio air temperature (°C)

Statistics	Jan	Feb	Mar	Apr	May	Jun	Jul	Aug	Sep	Oct	Nov	Dec
Mean	10.19	12.72	15.78	20.23	24.22	27.38	28.90	28.77	26.12	21.36	15.58	11.72
n	31	31	31	31	31	31	31	31	31	31	31	31
σ	2.18	3.59	3.07	1.62	1.37	1.18	1.24	1.08	1.26	1.35	1.81	2.13
C.V.	21	28	19	8	6	4	4	4	5	6	12	18
Minimum	6.02	8.03	7.69	15.50	21.81	25.81	26.08	26.49	22.09	16.07	10.92	6.19
Maximum	13.71	16.73	19.47	22.68	27.83	30.28	31.31	30.84	28.13	23.55	18.62	15.58
Median	10.54	12.68	16.51	20.62	23.90	27.07	29.14	28.93	25.97	21.59	15.63	11.67
25th %tile	8.85	11.81	15.04	19.50	23.34	26.49	28.06	28.05	25.70	20.81	14.31	10.73
75th %tile	11.60	13.80	17.55	21.04	24.74	27.91	29.59	29.34	27.01	21.92	16.97	13.06

San Antonio dew point temperature (°C)

Statistics	Jan	Feb	Mar	Apr	May	Jun	Jul	Aug	Sep	Oct	Nov	Dec
Mean	3.40	5.18	8.43	12.70	17.76	20.48	20.76	20.56	18.61	14.06	8.78	4.91
n	31	31	31	31	31	31	31	31	31	31	31	31
σ	2.25	2.88	2.41	2.62	1.49	1.13	1.09	0.82	1.88	1.78	2.38	2.89
C.V.	66	56	29	21	8	6	5	4	10	13	27	59
Minimum	-0.02	1.78	4.12	6.69	14.73	18.62	17.92	18.72	14.70	10.80	4.46	-2.33
Maximum	8.35	7.72	13.27	17.00	20.16	23.24	23.57	22.01	22.02	17.01	13.29	11.13
Median	3.86	5.24	8.53	13.44	18.11	20.70	20.73	20.60	18.80	14.06	9.04	4.97
25th %tile	1.11	4.01	6.80	11.12	16.70	19.60	20.07	19.99	17.24	12.67	6.76	3.30
75th %tile	4.91	6.41	10.27	14.47	18.76	21.33	21.46	21.21	19.81	15.53	9.92	6.68

San Antonio wind speed (m s⁻¹)

Statistics	Jan	Feb	Mar	Apr	May	Jun	Jul	Aug	Sep	Oct	Nov	Dec
Mean	3.78	3.96	4.36	4.30	4.16	4.19	4.10	3.68	3.66	3.73	3.72	3.62
n	31	31	31	31	31	31	31	31	31	31	31	31
σ	0.61	0.99	0.67	0.75	0.77	0.73	0.59	0.57	0.68	0.64	0.56	0.49
C.V.	16	25	15	17	18	17	14	16	19	17	15	13
Minimum	2.48	2.35	3.12	2.72	2.78	2.38	2.65	2.22	2.16	2.59	2.74	2.61
Maximum	5.02	5.14	5.38	5.77	5.72	5.15	5.30	4.49	4.87	5.01	4.80	4.46
Median	3.79	4.07	4.50	4.44	4.22	4.46	4.04	3.76	3.63	3.80	3.79	3.64
25th %tile	3.40	3.54	3.81	3.72	3.62	3.67	3.72	3.20	3.18	3.26	3.27	3.35
75th %tile	4.22	4.61	4.88	4.85	4.72	4.74	4.43	4.12	4.08	4.23	4.06	3.96

San Antonio precipitation (mm)

Statistics	Jan	Feb	Mar	Apr	May	Jun	Jul	Aug	Sep	Oct	Nov	Dec
Mean	39.9	45.8	49.3	65.8	122.9	102.0	50.6	67.3	76.2	96.2	57.3	48.3
n	31	31	31	31	31	31	31	31	31	31	31	31
σ	35.7	53.8	39.1	51.9	84.0	77.6	62.0	66.1	68.6	95.6	43.9	68.6
C.V.	90	118	79	79	68	76	123	98	90	99	77	142
Minimum	0.0	0.3	1.0	1.3	8.4	13.2	0.0	0.3	1.3	2.8	0.3	2.3
Maximum	143.3	161.8	155.4	223.5	326.4	303.5	210.6	283.0	332.5	459.0	152.7	354.6
Median	29.0	34.8	40.1	55.4	111.0	72.6	26.9	53.1	53.6	78.0	60.2	27.7
25th %tile	16.9	18.3	23.1	30.0	62.5	38.2	6.5	28.3	31.0	25.5	18.2	9.9
75th %tile	49.9	67.8	66.0	87.5	163.2	143.0	59.2	72.4	104.3	135.4	82.7	58.3

Boerne air temperature (°C)

Statistics	Jan	Feb	Mar	Apr	May	Jun	Jul	Aug	Sep	Oct	Nov	Dec
Mean	8.37	10.64	14.51	18.46	22.29	25.68	27.17	27.13	24.56	19.49	13.72	9.77
n	31	31	30	31	31	31	31	31	31	30	31	31
σ	2.09	3.58	3.17	1.23	1.26	1.06	0.91	0.92	1.15	1.27	1.86	1.94
C.V.	25	34	22	7	6	4	3	3	5	7	14	20
Minimum	3.89	6.06	10.89	16.00	20.11	24.00	24.50	24.83	21.39	14.67	10.11	4.50
Maximum	11.88	14.33	18.33	21.00	24.94	28.28	28.94	28.56	27.06	21.50	17.11	14.11
Median	8.61	10.50	14.58	18.39	22.11	25.61	27.17	27.44	24.56	19.58	14.11	10.00
25th %tile	7.08	9.67	13.68	17.92	21.42	24.83	26.72	26.50	24.06	19.06	12.14	9.00
75th %tile	9.64	11.44	15.50	19.17	23.08	26.39	27.67	27.78	25.33	20.32	15.11	10.69

LITERATURE CITED

Allen, R. G., L. S. Pereira, D. Raes, and M. Smith. 1998. Crop evapotranspiration -guidelines for computing crop water requirements - FAO irrigation and drainage paper 56. Food and Agriculture Organization of the United Nations.

Chapra, S.C. 1997. Water quality modeling. McGraw-Hill.

DeStasio, B. T., Jr., D. K. Hill, J. M. Kleinhans, N. P. Nibbelink, and J. J. Magnuson. 1996. Potential effects of global climate change on small north-temperate lakes: Physics, fish, and plankton. *Limnol. Oceanogr.* 41: 1136-1149.

Dutton, J. A., and R. A. Bryson. 1962. Heat flux in Lake Mendota. *Limnol. Oceanogr.* 7: 80-97.

Edinger, J. E., D. W. Duttweiler, and J. C. Geyer. 1968. The response of water temperature to meteorological conditions. *Water Resour. Res.* 4: 1137-1143.

- Fee, E. J., R. E. Hecky, S. E. M. Kasian, and D. R. Cruikshank. 1996. Effects of lake size, water clarity, and climatic variability on mixing depths in Canadian Shield lakes. *Limnol. Oceanogr.* 41: 912-920.
- Ford, D. E. 1990. Reservoir transport processes, p. 15-42. *In* K. W. Thornton, B. L. Kimmel, and F. E. Payne [eds.], *Reservoir limnology: ecological perspectives*. John Wiley & Sons.
- Ford, D. E., and M. C. Johnson. 1983. An assessment of reservoir density currents and inflow processes. Technical report E-83-7. U. S. Army Corps of Engineers.
- Groeger, A. W., and B. L. Kimmel. 1984 . Organic matter supply and processing in lakes and reservoirs, p. 282-285. *In* *Lake and reservoir management*. Proc. North American Lake Management Society Symposium. EPA 440/5/84-001.
- Groeger, A. W., and T. E. Tietjen. 1998. Hydrological and thermal regime in a subtropical reservoir. *Internat. Rev. Hydrobiol.* 83:83-92.
- Hambright, K. D., M. Gophen, and S. Serruya. 1994. Influence of long-term climate changes on the stratification of a subtropical, warm monomictic lake. *Limnol. Oceanogr.* 39: 1233-1242.

- Horne, A. G., and C. G. Goldman. 1994. *Limnology*. McGraw-Hill.
- Hostetler, S.W. 1995 . Hydrological and thermal response of lakes to climate: description and modeling, p. 63-82. *In* A. Lerman, D. Imboden, and J. Gat [eds.], *Physics and chemistry of lakes*, 2nd edition. Springer.
- Johnson, M. C., and D. E. Ford. 1987. The thermal structure and characteristics of DeGray lake, p. 168-187. *In* R. H. Kennedy and J. Nix [eds.], *Proceedings of the deGray lake symposium*. Technical Report E-87-4. US Army Corps of Engineers.
- Johnson, N. M., J. S. Eaton, and J. E. Richey. 1978. Analysis of five North American lake ecosystems II. Thermal energy and mechanical transfer. *Verh. Internat. Verein. Limnol.* 20:562-567.
- Johnson, N. M. and D. H. Merritt. 1979. Convective and advective circulation of Lake Powell, Utah-Arizona, during 1972-1975. *Water Resour. Res.* 15:873-884.
- Johnson, N. M., Likens, G. E., and J. S. Eaton. 1985. Stability, circulation and energy flux in mirror lake, p. 108-127. *In* G. E. Likens [ed.], *An ecosystem approach to aquatic ecology: mirror lake and its environment*. Springer-Verlag.

- Koberg, G. E. 1964. Methods to compute long wave radiation from the atmosphere and reflected solar radiation from a water surface. Prof. Paper 272-F, Geol. Surv., U. S. Dept. Interior.
- NOAA. 1969-1999. Climatological data- Texas. Vol. 74-104. National Oceanographic and Atmospheric Administration
- NOAA. 1991-1999. Local climatological data monthly summary: WBAN # 12921. National Oceanographic and Atmospheric Administration.
- Norwine, J. 1995. The regional climate of south Texas: patterns and trends, p. 138-155. *In* J. Norwine, J. R. Giardino, G. R. North, and J. B. Valdes [eds.], *The changing climate of Texas: predictability and implications for the future*. Cartographics.
- Owens, E. M. 1998. Thermal and heat transfer characteristics of Cannonsville Reservoir. *Lake and Reserv. Manage.* 14: 152-161.
- Owens, E. M., R. K. Gelda, S. W. Effler, and J. M. Hassett. 1998. Hydrologic analysis and model development for Cannonsville Reservoir. *Lake and Reserv. Manage.* 14: 140-151.
- Ragotzkie, R. A. 1978 . Heat budgets in lakes, p. 1-19. *In* A. Lerman [ed.], *Lakes: chemistry, geology, physics*. Springer-Verlag.

Schindler, D. W., S. E. Bayley, B. R. Parker, K. G. Beaty, D. R. Cruikshank, E. J.

Fee, E. U. Schindler, and M. P. Stainton. 1996. The effects of climatic warming on the properties of boreal lakes and streams at the Experimental Lakes Area, northwest Ontario. *Limnol. Oceanogr.* 41: 1004-

1017.

SPSS. 1998. SPSS Base 8.0. Statistical package for the social sciences, Inc.

Townsend, S. A., J. T. Luong-van, and K. T. Boland. 1996. Retention time as a primary determinant of colour and light attenuation in two tropical

Australian reservoirs. *Freshwat. Biol.* 36: 57-69.

Townsend, S. A., K. T. Boland, and J. T. Luong-van. 1997. Wet and dry season

heat loss in two tropical Australian reservoirs. *Arch. Hydrobiol.* 139: 51-68.

Turner, R. R., E. A. Laws, and R. C. Harris. 1983. Nutrient retention and

transformation in relation to hydraulic flushing rate in a small

impoundment. *Freshwat. Biol.* 13: 113-127.

USGS. 1969-1999. Water resources data-Texas. Water Resources Division, US

Geological Survey.

Vollenwieder, R. A. 1976. Advances in defining critical loading levels for

phosphorus in lake eutrophication. *Mem. Ist. Ital. Idrobiol.* 33: 53-83.

Wetzel, R. G., and G. E. Likens. 1991. The heat budgets of lakes, p. 43-53. *In* Limnological analyses. Springer-Verlag.

Wright, J. C. 1967. Effects of impoundments on production, water chemistry and heat budgets of rivers, p. 188-199. *In* Reservoir fishery resources symposium. American Fisheries Society.